

Bayesian Generalized Distributed Lag Regression with Variable Selection

Daniel Dempsey and Jason Wyse

School of Computer Science and Statistics, Trinity College Dublin

March 2024

Abstract

Distributed Lag Models (DLMs) and similar regression approaches such as MIDAS have been used for many decades in econometrics, and more recently in the study of air quality and its impact on human health. They are useful not only for quantifying accumulating and delayed effects, but also for estimating the lags that are most susceptible to these effects. Among other things, they have been used to infer the period of exposure to poor air quality which might negatively impact child birth weight. The increased attention DLMs have received in recent years is reflective of their potential to help us understand a great many issues, particularly in the investigation of how the environment affects human health. In this paper we describe how to expand the utility of these models for Bayesian inference by leveraging latent-variables. In particular we explain how to perform binary regression to better handle imbalanced data, how to incorporate negative binomial regression, and how to estimate the probability of predictor inclusion. Extra parameters introduced through the DLM framework may require calibration for the MCMC algorithm, but this will not be the case in DLM-based analyses often seen in pollution exposure literature. In these cases, the parameters are inferred through a fully automatic Gibbs sampling procedure.

Keywords: Distributed lag regression, Polya-Gamma regression, Functional data analysis, Air quality, Pollution exposure, Environmental modelling.

1 Introduction

It can often be the case that variables are interconnected or correlated in a manner that accumulates over time. For example, the extent to which exposure to poor air quality affects human health will depend on both the concentration of poor quality air and the length of time an individual was exposed to it. There are likely to be temporal windows of exposure that will more directly impact current health status than others. A basic assumption along these lines is that

the effect of exposure will asymptotically (in time) decline, though of course there is no guarantee that the decline is monotonic, at least in the short term. Understanding these temporal ‘profiles’ of exposure is key to understanding the effects of these exposures as a whole. *Distributed Lag Models* (DLMs) can help us understand these exposure profiles by applying weights to the temporal lags of the covariates corresponding to the degree to which they contribute the predictor’s effect on the response variable.

Distributed lags were introduced by [Almon \(1965\)](#) and were most strongly associated with econometrics for many of the intervening decades. See for example [Hannan \(1965\)](#), [Chen et al. \(1972\)](#), [Sims \(1971\)](#) and [Dhrymes \(1981\)](#) for some early examples. A related class of models known as *Mixed Data Sampling* (MIDAS) models were introduced by [Ghysels et al. \(2004\)](#) to resolve the issue of analysing data of mixed sampling regimes (for example, measuring the association of a time series with observations sampled yearly and another with observations sampled monthly). This too was mainly in service of econometrics. In recent years, DLMs have been used to investigate the impact of the environment on different aspects of human health. This appears to have been popularised by [Schwartz \(2000\)](#) who implemented a DLM into a generalised additive model ([Hastie and Tibshirani, 1987](#)) to analyse how daily death count is correlated with exposure to poor air quality. A similar study was performed later by [Zanobetti et al. \(2002\)](#).

The utility of DLMs (and MIDAS) is evident from the number of analyses centered around them; [Wilson et al. \(2017\)](#) used a Bayesian DLM to investigate the relationship between air quality and adverse health outcomes of newborns. [Warren et al. \(2020\)](#) implemented random effects to account for spatial autocorrelation into their DLM when they investigated the effect of air quality exposure during pregnancy and the birth weight of newborns. [Clements and Galvão \(2008\)](#) suggest how to safely incorporate auto-regression terms into MIDAS models. [Xu et al. \(2019\)](#) synthesised the MIDAS model with an artificial neural network model for very flexible non-linear fits. [Li et al. \(2021\)](#) took this a step further by incorporating the effects of temporal correlation. [Antonelli et al. \(2021\)](#) developed a Bayesian DLM that utilises spike-and-slab priors for variable selection ([Mitchell and Beauchamp, 1988](#)). [Mogliani and Simoni \(2020\)](#) similarly suggests a MIDAS model with spike-and-slab priors, but with a Laplacian distribution for the slab to incorporate Bayesian Group-LASSO variable selection ([Meier et al., 2008; Xu and Ghosh, 2015](#)). [Mork et al. \(2021\)](#) combines DLMs with Bayesian additive regression trees ([Chipman et al., 2010](#)) to analyse the relationship between air quality exposure and the weight of newly born children.

In this article we demonstrate how to perform Bayesian regression for generalised DLF models with particular focus paid to the negative binomial and binary quantile models. Depending on the exact specifications of the DLM (to be discussed later), Markov Chain Monte Carlo (MCMC) implementation of these models are fully automatic beyond setting priors and starting values. As

has become common for Bayesian GLMs since [Albert and Chib \(1993\)](#), these methods are facilitated by the incorporation of latent variables for their ease of implementation. The latent variable approaches we adopt can be leveraged to infer the posterior probability of particular exposures having an impact on health or other indicators.

The remainder of the article is laid out as follows. In section 2 we present the general framework for generalised DLMs, focusing on how we can apply binary quantile regression and negative binomial regression in particular. We outline a simulation study in section 3 for assessing the accuracy of the methods at estimating associated parameters and how well the variable selection procedure performs. There is an extra document supplementary to this manuscript that contains further simulation study results (via visualisations) than what is presented here. In section 4 the proposed approach is demonstrated on a real data example. Both the real and simulated data examples are based on Chicago air quality data available in the `dlnm` package for R ([Gasparrini, 2011](#)). We conclude in section 5 with a description of merits and possible extensions of the work.

2 Methods

Denote the vector response variables as \mathbf{y} . We want to model its association with a collection of predictors, some of which have a ‘standard’ *contemporaneous* effect on the response (referred to as *static* predictors), but others that we believe have a lagged effect on the response which is modulated by the dosage or duration of exposure to the longitudinal predictor (referred to as *dynamic* predictors). For example, measuring how the exposure to bad air quality affects respiratory function. We need to measure the effect of bad air quality as in standard regression problems, but now we also need to infer how that effect is distributed over its longitudinal units, usually time. The relationship between the lags of the dynamic predictors and the response will be referred to as the *lag-response* model. DLMs are regression methods built specifically to handle these kinds of problems.

We will denote the matrix of dynamic predictors as \mathbf{Z} and the static predictors (including the intercept, if used) as \mathbf{Z}_S . Under this notation, DLMs can be expressed in the following general form;

$$\mathbf{y} \sim F(g^{-1}(\boldsymbol{\eta}), \boldsymbol{\Phi}) \quad (1)$$

$$\boldsymbol{\eta} = \mathbf{Z}_S \boldsymbol{\beta}_S + \sum_{i=1}^p h_i(\mathbf{z}_i, \boldsymbol{\Theta}_i) \quad (2)$$

F is the assumed distribution of the response \mathbf{y} , $g^{-1}(\cdot)$ is the inverse link function that allows for generalised regression, and $\boldsymbol{\Phi}$ is the collection of parameters of F that are required alongside the transformed linear predictor. \mathbf{z}_i is the i^{th}

dynamic variable, or equivalently, the i^{th} column of the \mathbf{Z} matrix, $i = 1, \dots, p$. $\boldsymbol{\beta}_S$ is the vector of linear regression parameters corresponding to the static variables. Notice that if there are no dynamic predictors, this simply collapses to a standard GLM.

$h_i(\cdot)$ encodes the assumed nature of the lag-response of the i^{th} dynamic predictor, which will usually be further parameterised by $\boldsymbol{\Theta}_i$. This can be as simple as a crude aggregate over the lags (in which case there will be no $\boldsymbol{\Theta}_i$). Another option is to use a linear combination of the last τ lags (referred to as the *time window*) of the dynamic variables, effectively treating each lag as its own predictor. This is a conceptually simple way to model the lag-response but it is heavily parameterised with a large degree of co-linearity across the lag predictors. A common compromise in longitudinal health studies is to use a linear combination of a basis expansion of the lags (Gasparrini, 2011). Another option, commonly seen in the MIDAS literature, is to assign weights to the lags based on a (usually) parameterised curve. The weights are incorporated into the model through convolution, scaled by a linear coefficient;

$$h_i(\mathbf{z}_i, \boldsymbol{\Theta}_i) = \beta_i \sum_{k=0}^{\tau_i} w_i(k; \boldsymbol{\Theta}_i) Z_{t-k, i}$$

where $w_i(\cdot)$ is the function that assigns the weights, called a *distributed lag function* (DLF) with parameters $\boldsymbol{\Theta}_i$, and $Z_{i,j}$ denotes the i, j^{th} cell of matrix \mathbf{Z} .

The DLF can be any function that asymptotically declines to zero as the lags grow larger, but it must be constrained in some way to ensure the coefficient β_i is identifiable. A common constraint is $w_i(k, \boldsymbol{\Theta}_i) > 0$ for all k and $\sum_{k=1}^{\tau_i} w_i(k, \boldsymbol{\Theta}_i) = 1$. This particular approach is useful as it ensures that a dynamic variable can't swap between having positive *and* negative impacts on the value of the response (insofar that it has any impact at all) for different lags. A list of typical choices for DLFs are given in Table 1 of Ghysels et al. (2016).

While the DLF approach offers what appears to be a pleasing compromise between model flexibility and analyst control, the non-linear relationship between the values of \mathbf{y} and $\boldsymbol{\theta}$ can present challenges for inference and therefore requires special consideration in MCMC routines, such as extra Metropolis-within-Gibbs steps. By contrast, the linear combinations of the lags or basis expansions can easily be incorporated, as they require no further alterations of the methodologies we will discuss in the forthcoming sections.

2.1 Model Inference

Going back to (1), in this manuscript we are primarily concerned with the situation where F is a discrete distribution, used to model either count or binary responses. When estimating the posterior, straightforward application of Bayes' Theorem in either case leads to full conditionals that cannot be sampled directly regardless of the choice of prior. These are recognised as challenging modelling

problems for Bayesian methods. However, in both cases we can alleviate this issue with the introduction of latent variables. First let us introduce some extra notation; let β (with the subscript omitted), denote the vector containing β_S and the subset of all Θ_i that are linear coefficients. Similarly let \mathbf{X} be the column-wise concatenation of \mathbf{Z}_S and the vectors relating to the linear predictors of Θ_i . Note that, when using a linear combination of basis expansions as $h_i(\cdot)$ then β contains all regression parameters and \mathbf{X} contains all predictors.

2.1.1 Count Data Inference

Automatic Gibbs sampling for the parameters of the negative binomial regression model was explained by [Pillow and Scott \(2012\)](#) and [Zhou et al. \(2012\)](#), which is briefly summarised here. We start by assuming y_t (in this case a discrete count) follows a negative binomial distribution with probability parameter equal to the transformed linear predictor and unknown stopping parameter ξ ,

$$\begin{aligned} y_t &\sim \text{NB}(\xi, p_t) \\ p_t &= \frac{\exp(\eta_t)}{1 + \exp(\eta_t)} \end{aligned}$$

where η_t are the components of η given in (2). Assuming a Gaussian prior of mean vector \mathbf{m} and covariance matrix \mathbf{v} , exact and automatic Gibbs sampling from the posterior of β can be accomplished by introducing a latent variable ω that follows a Polya-Gamma distribution ([Polson et al., 2013](#)),

$$\begin{aligned} \omega_t | \beta, \xi &\sim \text{PG} \left(y_t + \xi, \mathbf{z}_{t,S}^\top \beta_S + \sum_{i=1}^p h_i(\mathbf{Z}_{t,i}, \Theta_i) \right) \\ \beta | \omega, \xi &\sim \text{N}(\mathbf{M}_C, \mathbf{V}_C) \\ \mathbf{V}_C &= (\mathbf{X}^\top \Omega_C \mathbf{X} + \mathbf{v}^{-1})^{-1} \\ \mathbf{M}_C &= \mathbf{V}_C (\mathbf{X}^\top \Omega_C \lambda_C + \mathbf{v}^{-1} \mathbf{m}) \\ \Omega_C &= \text{diag}(\omega) \\ \lambda_{t,C} &= (y_t - \xi) / 2\omega_t \end{aligned}$$

where $\text{diag}(\cdot)$ constructs a diagonal matrix based on the components of the vector input. The subscript C used throughout to highlight that these are the parameters corresponding to the count data model; this is to avoid notational conflict in the next section. Regarding the Polya-Gamma distribution sampling, section 4 of [Polson et al. \(2013\)](#) describes an exact and efficient rejection sampler which they have implemented in their R package `BayesLogit`.

To sample from the posterior of ξ , for conjugacy we assume a gamma distribution prior with shape and scale parameter a_0 and b_0 . We also need to include yet another latent variable ψ to the model. ξ is then updated as follows:

$$\begin{aligned}\pi(\psi_t = j \mid \xi) &= R_{y_t, j} \\ \xi &\sim \text{Gamma} \left(a_0 + \sum_{i=1}^N \psi_i, b_0 - \sum_{i=1}^N \ln(1 - p_t) \right)\end{aligned}$$

where N is the length of \mathbf{y} and $R_{i,j}$ is the i, j th element of the following (recursively constructed) lower triangular matrix:

$$R_{i,j} = \frac{i-1}{i} R_{i-1,j} + \frac{\xi}{i} R_{i-1,j-1} \quad (3)$$

with $R_{1,1} = R_{0,1} = 1$, and $R_{i,j} = 0$ when $j = 0$ or $j > i$. This matrix has square dimensions equal to the maximum value of \mathbf{y} . Construction of this matrix is the biggest potential source of computational bottleneck as it has to be re-done at every iteration, cell-by-cell. An alternative non-recursive method exists (Zhou et al., 2012) but it becomes numerically unstable as y_{\max} or ξ grow too large, so in general we recommend using (3).

Poisson regression can be approximated by simply fixing ξ to some large number but otherwise following the above approach, circumventing the need to compute (3). See D'Angelo and Canale (2022) for further notes on approximate Bayesian Poisson regression. Zhou et al. (2012) augmented the above algorithm to capture broader forms of variation, and also derived associated Variational Bayes estimates.

2.1.2 Possibly Imbalanced Binary Data Inference

Now let us assume y_t is binary. Exact Gibbs sampling for probit regression (and an approximation for logistic regression) via latent variables was first proposed by Albert and Chib (1993) and has become the blueprint for binary response regression; see Holmes and Held (2006); Frühwirth-Schnatter and Frühwirth (2010); Polson et al. (2013); Zens et al. (2023) for more examples of how it is applied for logistic regression. Here, we wish to use this same approach as a way of handling DLMs for binary responses, where the response may be imbalanced. This can occur in, say, medical studies where the focus is on rare diseases, symptoms or other health outcomes.

The logit link has been shown to result in bias of the MLE of the regression parameters when it misspecifies the ‘true’ link and that this bias is particularly diminished by skewness (Czado and Santner, 1992). For this reason, the approach we recommend here is binary quantile regression (Benoit and Van den Poel, 2012; Benoit and den Poel, 2017) using the 3-parameter *Asymmetric Laplace*

Distribution (ALD) (Yu and Zhang, 2005), which uses a parameter $q \in \{0, 1\}$ (corresponding to the desired quantile) that controls the degree of skew. When $q = 0.5$ it collapses to the standard (symmetric) Laplacian distribution. The ALD Bayesian quantile model is

$$\begin{aligned} y_t &= I(y_t^* > 0) \\ \mathbf{y}^* &= \mathbf{Z}_S \boldsymbol{\beta}_S + \sum_{i=1}^p h_i(\mathbf{z}_i, \boldsymbol{\Theta}_i) + \boldsymbol{\epsilon} \\ \boldsymbol{\epsilon}_t &\sim \text{ALD}(\mu = 0, \sigma = 1, q) \end{aligned}$$

where $I(\cdot)$ is equal to 1 if the condition inside the parenthesis is met and 0 otherwise. μ and σ are location and scale parameters for the ALD. Kozumi and Kobayashi (2011) found that the ALD can be expressed as scale-mixture of Gaussians, allowing us to form an algorithm for exact Gibbs sampling, though we exclude the details and derivations here. First we update the \mathbf{y}^* latent variable,

$$y_t^* | y_t, \boldsymbol{\beta}, \boldsymbol{\theta} \sim \begin{cases} \text{ALD}(\mathbf{x}_t^\top \boldsymbol{\beta}, \sigma = 1, q) & \text{restricted to the positive axis when } y_i = 1, \\ \text{ALD}(\mathbf{x}_t^\top \boldsymbol{\beta}, \sigma = 1, q) & \text{restricted to the negative axis when } y_i = 0. \end{cases}$$

This truncated ALD is easily sampled from using the inversion method, or via the approach proposed in section 4.2 of Benoit and den Poel (2017). Here we are jointly updating \mathbf{y} with another latent variable $\boldsymbol{\nu}$, whose full conditional distribution is a Generalised Inverse Gaussian distribution (Jorgensen, 2012),

$$\nu_t | y_t^*, \boldsymbol{\beta} \sim \text{GIG}(1/2, \chi_t^2, \delta^2)$$

where

$$\chi_t^2 = \frac{(y_t^* - \mathbf{x}_t^\top \boldsymbol{\beta})^2}{\phi^2}, \quad \delta^2 = 2 + \frac{\psi^2}{\phi^2}, \quad \psi^2 = \left(\frac{1-2q}{q(1-q)} \right)^2, \quad \phi^2 = \frac{2}{q(1-q)}.$$

The full conditional distribution of \mathbf{y} (including $\boldsymbol{\nu}$) is truncated Gaussian, but the joint update with $\boldsymbol{\nu}$ improves Monte Carlo efficiency.

As with negative binomial inference, the resulting full conditional distribution of the linear coefficients is Gaussian,

$$\boldsymbol{\beta} | \mathbf{y}, \boldsymbol{\theta}, \boldsymbol{\nu} \sim \text{N}(\mathbf{M}_B, \mathbf{V}_B)$$

where

$$\begin{aligned}
\mathbf{V}_B &= (\mathbf{X}^\top \boldsymbol{\Omega}_B \mathbf{X} + \mathbf{v}^{-1})^{-1} \\
\mathbf{M}_B &= \mathbf{V}_B (\mathbf{X}^\top \boldsymbol{\Omega}_B \boldsymbol{\lambda}_B + \mathbf{v}^{-1} \mathbf{m}) \\
\boldsymbol{\Omega}_B &= (\phi^2 \text{diag}(\boldsymbol{\nu}))^{-1} \\
\boldsymbol{\lambda}_B &= \mathbf{y}^* - \psi \boldsymbol{\nu}
\end{aligned}$$

and as before, \mathbf{m} and \mathbf{v} are the mean and covariance of the prior Gaussian distribution for $\boldsymbol{\beta}$.

In the event that $h(\cdot)$ from equation (1) is chosen in such a way that all the $\boldsymbol{\Theta}_i$ are parameters for linear predictors, then this is all that is necessary for fitting DLMs with count or binary responses. As stated before, any non-linear parameters that arise from the lag-response model (as usually seen when applying DLFs) will require further consideration.

2.2 Covariate Inclusion Inference

Let $\gamma_i \in \{0, 1\}$ represent whether or not a corresponding predictor (or groups of predictors) be included in the model. Regardless of which of the above models we use, the approach of inferring the posterior of $\boldsymbol{\gamma}$ is the same. [Holmes and Held \(2006\)](#) suggest we update $\boldsymbol{\gamma}$ jointly with $\boldsymbol{\beta}$ through a Metropolis update,

$$q(\boldsymbol{\beta}^*, \boldsymbol{\gamma}^*) = \pi(\boldsymbol{\beta}^* | \boldsymbol{\gamma}^*, \mathcal{D}) q(\boldsymbol{\gamma}^* | \boldsymbol{\gamma})$$

where \mathcal{D} denotes every parameter in the model (including latent variables). The first component is simply the full conditional distribution of $\boldsymbol{\beta}$ already derived for both models above, but only using the columns of \mathbf{X} supported by $\boldsymbol{\gamma}^*$. The second is the user-chosen method for proposing new values of $\boldsymbol{\gamma}$. Under this proposal scheme, the acceptance rate α is

$$\alpha = \min \left\{ 1, \frac{|\mathbf{v}_{\boldsymbol{\gamma}^*}|^{-0.5} |\mathbf{V}_{\boldsymbol{\gamma}^*}|^{0.5} \exp [0.5 (\mathbf{M}_{\boldsymbol{\gamma}^*}^\top \mathbf{V}_{\boldsymbol{\gamma}^*}^{-1} \mathbf{M}_{\boldsymbol{\gamma}^*} + \mathbf{m}_{\boldsymbol{\gamma}^*}^\top \mathbf{v}_{\boldsymbol{\gamma}^*}^{-1} \mathbf{m}_{\boldsymbol{\gamma}^*})] q(\boldsymbol{\gamma} | \boldsymbol{\gamma}^*) \pi_{\boldsymbol{\gamma}}(\boldsymbol{\gamma}^*)}{|\mathbf{v}_{\boldsymbol{\gamma}}|^{-0.5} |\mathbf{V}_{\boldsymbol{\gamma}}|^{0.5} \exp [0.5 (\mathbf{M}_{\boldsymbol{\gamma}}^\top \mathbf{V}_{\boldsymbol{\gamma}}^{-1} \mathbf{M}_{\boldsymbol{\gamma}} + \mathbf{m}_{\boldsymbol{\gamma}}^\top \mathbf{v}_{\boldsymbol{\gamma}}^{-1} \mathbf{m}_{\boldsymbol{\gamma}})] q(\boldsymbol{\gamma}^* | \boldsymbol{\gamma}) \pi_{\boldsymbol{\gamma}}(\boldsymbol{\gamma})} \right\}$$

where $\pi_{\boldsymbol{\gamma}}(\cdot)$ is the prior of $\boldsymbol{\gamma}$ and $q(\boldsymbol{\gamma})$ is the proposal distribution. Here, $\mathbf{M}_{\boldsymbol{\gamma}}$ and $\mathbf{V}_{\boldsymbol{\gamma}}$ correspond to the mean and variance of the full conditional distribution of $\boldsymbol{\beta}$ for the model described by $\boldsymbol{\gamma}$. Notice that, as written, $\boldsymbol{\beta}$ is marginalised so no further adjustments to the acceptance probability is required. This makes sense as ‘removing’ a variable from the above regression methods is the same as simply fixing its associated slope at zero, so there is actually no shift in the dimensionality when any element of $\boldsymbol{\gamma}$ is altered. This is obviously no longer the case if $h(\cdot)$ is a DLF (or similar), in which case altering $\boldsymbol{\gamma}$ will now result

in genuine dimension jumping and the acceptance rate will need to be adjusted accordingly (Green, 1995; Green and Hastie, 2009).

In regards to the proposal $q(\gamma)$, the approach we assume for the rest of this paper is that, for each MCMC iteration, one random element from γ is chosen to be swapped from 0 to 1 or vice-versa. This is a symmetric proposal, so the $q(\cdot)$ terms cancel in the acceptance probability equation. Note this becomes unsuitable as the number of potential predictors grow larger since the probability that any specific value is swapped at any iteration shrinks to zero. Adapting a horseshoe prior (Carvalho et al., 2010; Piironen and Vehtari, 2017) can be beneficial in such situations.

3 Simulation Study

A simulation study was performed to test the above methods. The simulated data are partially based on a table of air quality metrics collected between 1987 and 2000 in Chicago, available through the R package `dlnm` (Gasparrini, 2011). Three columns from this dataset are used as dynamic predictors: mean relative humidity, PM10, and ozone (O3). Two further static variables are generated by taking the absolute value of draws from the standard normal distribution. The full Chicago data has 5114 observations; we will use the full dataset for one set of simulations, whereas we will only use the first 250 observations for another. Some humidity and PM10 values in the dataset are missing; these are imputed via predictive mean matching using the `mice` package in R (van Buuren and Groothuis-Oudshoorn, 2011).

The lag-response relationship between the real dynamic variables and the simulated response were as follows: humidity had a unimodal delayed effect, PM10 had a linearly decreasing effect, and O3 had a bimodal effect. The delayed and bimodal effects were created using a 2 degree exponential polynomial (Almon, 1965):

$$w(k, \boldsymbol{\theta}) \propto \exp(\theta_1 k + \theta_2 k^2) \quad (4)$$

where $w(\cdot, \cdot)$ is scaled across all lags k within each time window such that $\sum_{k=0}^{\tau} w(k, \boldsymbol{\theta}) = 1$. This is so the lag-response can be interpreted as a weighted average over the lags (the same scaling also applies for the linear decreasing lag-response). For the delayed effect, we use $\boldsymbol{\theta} = \{0.32, -0.02\}$. For the bimodal effect we combine two Almon functions w_1 and w_2 with $\boldsymbol{\theta}_1 = \{0.2, -0.03\}$ and $\boldsymbol{\theta}_2 = \{6, -0.1\}$. We then take the effect to be $0.7w_1 + 0.3w_2$. The resultant lag response profiles are shown as the dashed blue lines in Figure 1.

The overall effect sizes were set as follows: the two static variables have an overall effect of -0.5 and 0.01 . Humidity, PM10 and ozone had overall effects sizes (of their lag-response relationships) of 0.5 , 0.01 , and -0.5 respectively. This gives us a mix of strong and weak effects to test the variable selection

scheme. Lag-responses were modelled using cubic b-splines with three evenly spaced knots.

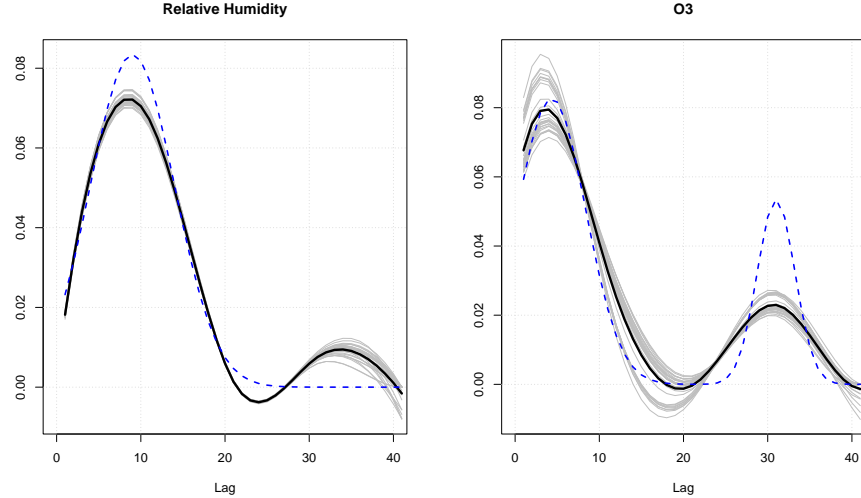
Datasets were created with both a count response and a binary response. The count response simulations used the negative binomial distribution with stopping parameter equal to 50, and intercept equal to -1 . The binary response simulations were simulated by drawing random values from the ALD with the skew parameter equal to 0.9 and setting the intercept of the regression model to 0, with the binary response then being set to 1 for positive values and 0 otherwise.

In summation, there are four distinct types of simulations; Large/small datasets with count/binary responses. Four of each dataset was created, and for each of these datasets we fit the appropriate model 30 times to assess the Monte Carlo consistency. For brevity only one set of the large simulations (for both count and binary simulations) will be discussed in this manuscript; see Figures 1–4. Relevant visualisations for *all* simulation tests are compiled in the supplementary document.

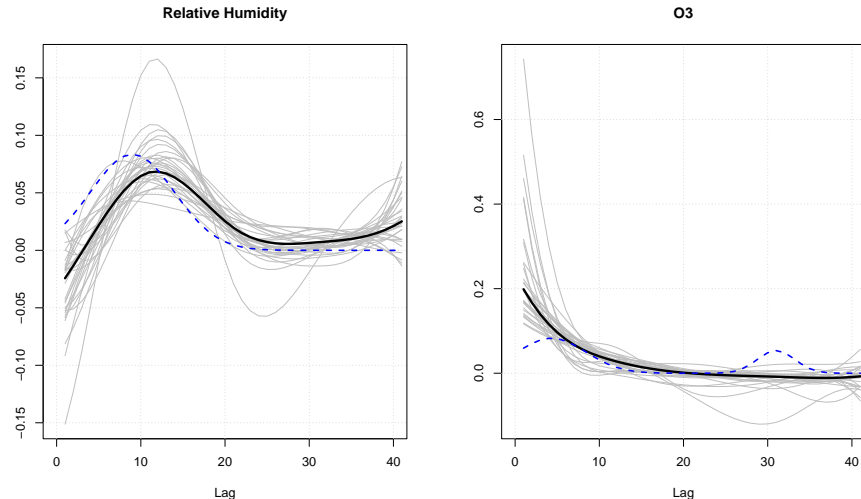
From Figure 1 we see that the MCMC routine was able to accurately infer the lag-response relationship for relative humidity and ozone for the count-response data. Binary simulations were somewhat less successful; the lag-response relationship with relative humidity, while overall accurate, is less consistent, and the algorithm failed to pick up the smaller mode for the ozone lag-response relationship. PM10 was omitted as the overall effect is so small that the lag-response is ill-defined and thus expected to fail. However the attempt at the estimation is shown in the supplementary materials.

Figure 2 shows the variable inclusion parameters. The weaker effects are largely discarded from the model with a high degree of certainty. More interestingly, we see that γ are discarding individual b-spline components even from the non-zero effects. This behaviour could be potentially leveraged to inform about the parameters of the b-spline construction (knots, component polynomial degree, etc). The binary response simulations, while performing still well overall, display a lack of sampling consistency, especially with the ozone variable.

The difference between estimated and true effect sizes are shown in Figure 3. We see that the effects were mostly accurate, though some effects were overestimated, in particular the intercept and humidity slope in the negative binomial simulations. The other simulations we performed, shown in the supplementary materials, show further varying degrees of over/under estimation for some dynamic effects for both count and binary response simulations. By contrast, the static effects (apart from the intercept) are almost always very accurate with a high degree of Monte Carlo consistency. But these are simply regression slopes; on the other hand, dynamic effects are intertwined with lag-response estimation, increasing the statistical complexity which likely accounts for the poorer performance. Another thing worth pointing out here are the differences in the count and binary simulations - as before, imbalanced binary response is harder

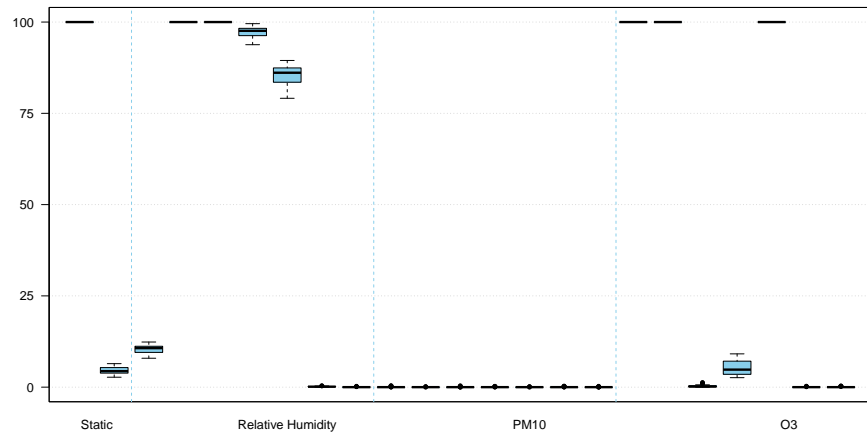


(a) Count data simulation results.

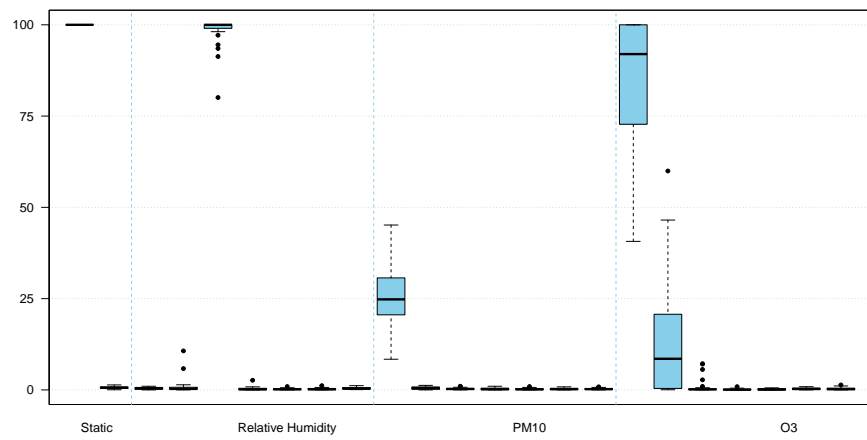


(b) Binary data simulation results.

Figure 1: Estimated lag-responses for simulated data compared to their true values. Grey lines represent each of the 30 MCMC runs, the thick black line is the average across all runs, and the blue dashed lines are the correct values. The correct values are the same for both groups, they only appear different here due to the differing scales of the y-axes. PM10 is omitted here as its small effect size means that its associated lag-response is ill-defined, though it is included in the supplementary results.

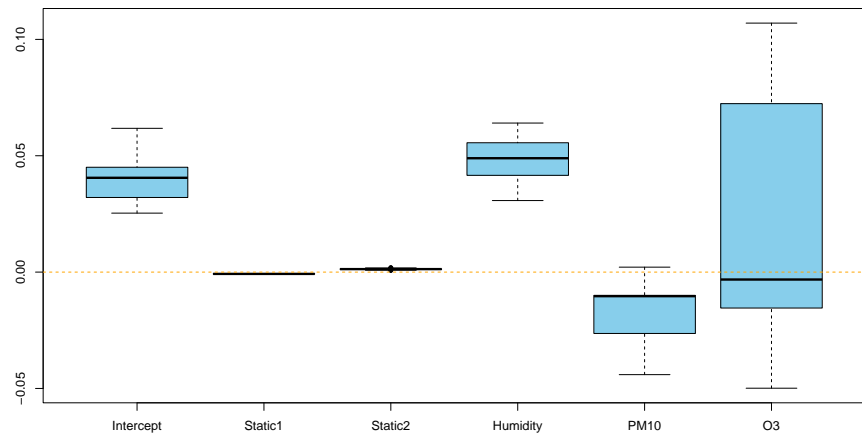


(a) Count data simulation results.

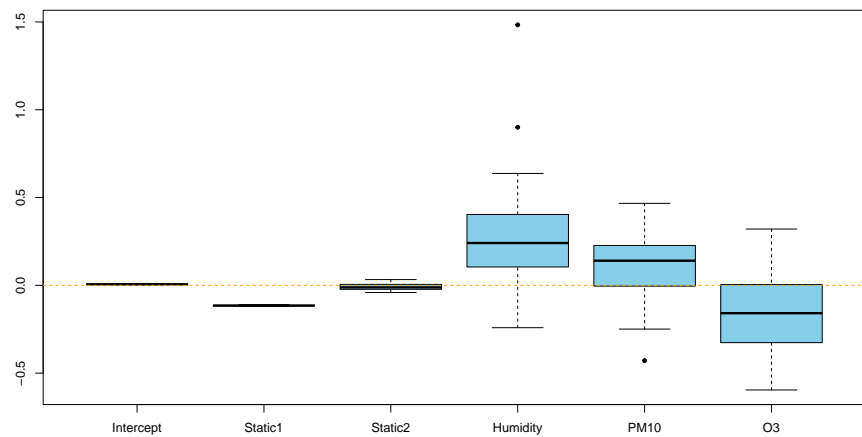


(b) Binary data simulation results.

Figure 2: Covariate inclusion posteriors for simulated data across all 30 MCMC runs (intercept omitted).



(a) Count data simulation results.



(b) Binary data simulation results.

Figure 3: The difference between the mean estimated effect sizes and their true values for simulated data across all 30 MCMC runs. Note that the y-axes of the above graphs are on different scales.

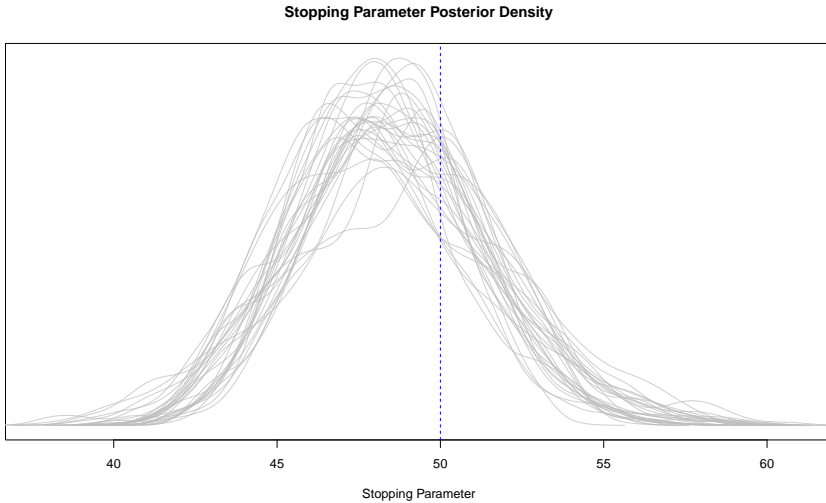


Figure 4: Posterior of the negative binomial stopping parameter for simulated data. Each grey line represents a posterior from one of the thirty MCMC runs. The blue dashed line denotes the true value.

to infer from (note the difference in y-axes scales in Figure 3).

Finally, 4 displays the density plot of the MCMC posterior samples of the negative binomial stopping parameter. The Monte Carlo posterior mode tends to slightly underestimate, but the true value still sits comfortably within high posterior density regions.

Overall, we would say the algorithms perform well, especially for the count simulations. The fact that binary regression performs somewhat worse is understandable given that binary data carries less information to infer from - especially when imbalanced, as is the case for these simulations.

4 Chicago Air Quality Data

We fit DLM models to the Chicago air quality dataset that was used to partially simulate response data in the previous section. This data was originally part of the National Morbidity, Mortality and Air Pollution Study database, but to our knowledge the full dataset is no longer available. The data we use here is available through the *dlnm* package (Gasparrini, 2011). In addition to the relative humidity, PM10 levels, and ozone levels that we spoke of in the simulation section, the full dataset has two more environmental variables: mean daily temperature and dew point temperature, both of which are heavily correlated (Pearson ≈ 0.95). It also records the day of the week and the month of the year the air quality metrics were recorded. Month of the year is obviously useful for

coding seasonality, and day of week is also known to have an impact on daily reported numbers due to the nature of healthcare surveillance (Buckingham-Jeffery et al., 2017). Day of the week will be dummy-encoded and included in the model (Sunday excluded). The months were aggregated into their respective seasons, which was dummy encoded and included in the model (Autumn excluded).

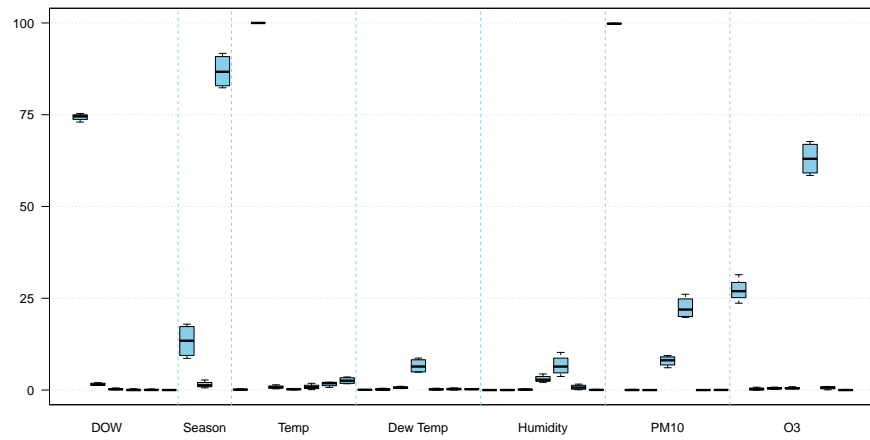
There are three different measures of daily death rates in the data: the number of cardiovascular-related deaths, the number of respiratory related deaths, and the overall number of non-accidental deaths. The daily overall death rate was chosen as the response; the others were discarded. Missing values are imputed using predictive mean matching via the `mice` package (van Buuren and Groothuis-Oudshoorn, 2011) with default settings.

The remaining air quality metrics are included as dynamic variables. In each case we assume a lag length of 40 days, and the lag-response are modelled using cubic b-splines with 3 evenly spaced knots.

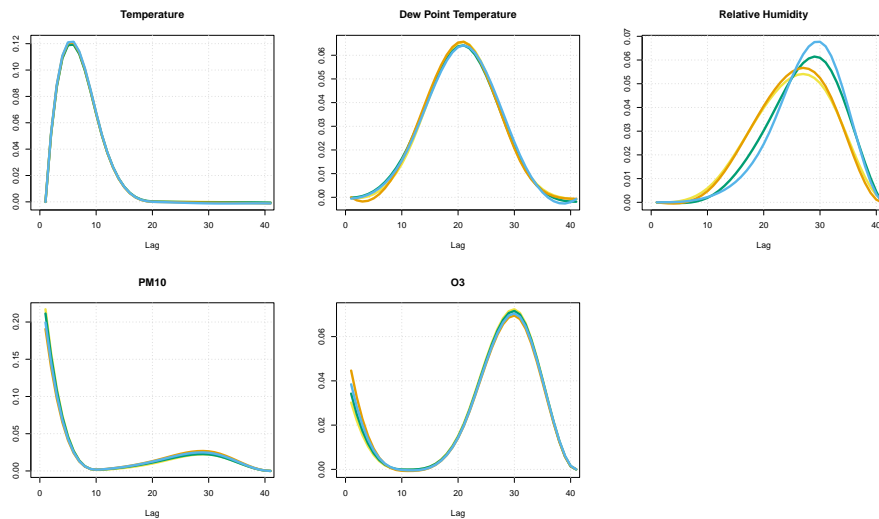
We fit a negative binomial DLM to the dataset as described. We also fit a binary quantile regression DLM to the dataset by dichotomising the response variable; any day that had in excess of 135 deaths (roughly 10% of the data) was assigned a value of 1, and 0 otherwise. Please note that we are not condoning dichotomisation for serious analysis of this data or others - this was done purely for illustrative purposes.

For the MCMC fits shown, we adopt independent Gaussian distributions centered at 0 with variance 100 as priors for the regression coefficients. We use a Bernoulli distribution with probability parameter equal to 0.5 as prior for each of the variable inclusion parameters. A Gamma distribution with shape and rate equal to 2 and 1/50 respectively was used for the stopping parameter prior. We run the MCMC algorithm 4 times each with their own starting values. One run starts with the intercept only model, another starts at the full inclusion model, and the other two use random starts; each non-intercept predictor is included with probability 0.5. They are all ran for 10^5 iterations, half of which is discarded, and only every 10th value is retained thereafter.

The posterior of the covariate inclusion parameters and the means of the estimated lag-response relationships are given in Figures 5 and 6. The negative binomial DLM shows very consistent results for both the inclusion indicators and the lag-responses, even with the large degree of multicollinearity between temperature and dew-point temperature. There was more uncertainty within the quantile regression results, as is expected due to binary imbalance. Both models tend to agree on what variables should be included, with relatively strong levels of inclusion for temperature, PM10, and ozone. There's some agreement with the estimated lag-responses too; PM10 has a 7-day delayed effect on death rates, PM10 has an immediate effect followed by a sharp decline, and ozone has both an immediate effect and a 30-day delayed effect on death rates. They both disagree on the relationship between death rates and dew point tempera-

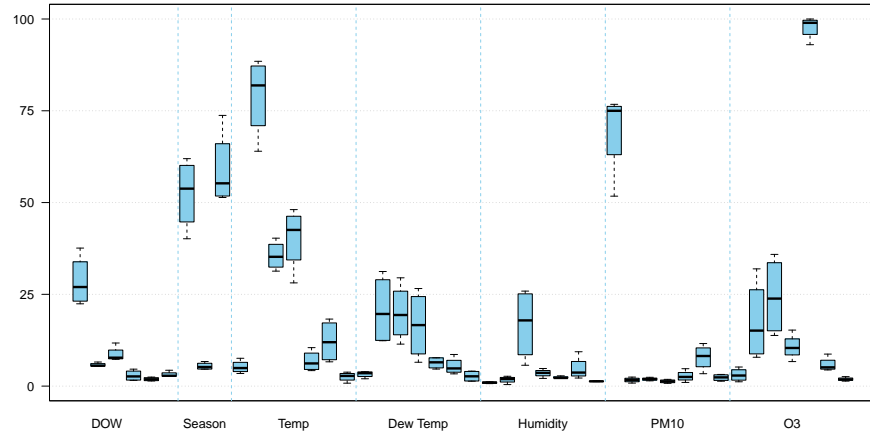


(a) Covariate inclusion posterior across all 4 runs.

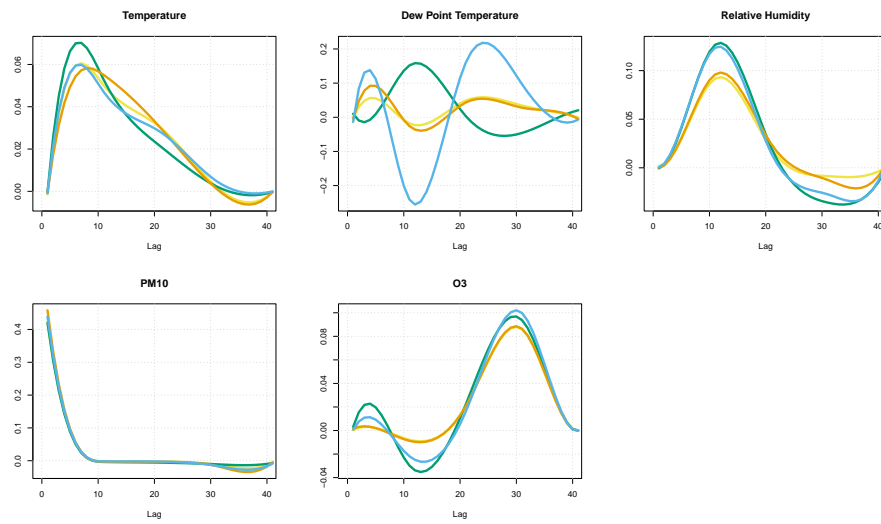


(b) Monte Carlo means of the response-lag relationship for all 4 runs.

Figure 5: Results from the negative binomial fit of the Chicago air quality data.



(a) Covariate inclusion posterior across all 4 runs.



(b) Monte Carlo means of the response-lag relationship for all 4 runs.

Figure 6: Results from the binary quantile regression fit of the Chicago air quality data.

ture and humidity, though the models agreed that these predictors were mostly irrelevant regardless.

5 Conclusion

Latent variables are frequently leveraged when fitting Bayesian GLMs (especially binary response models) as they result in fully tractable conditional distributions and require no further tuning beyond setting priors and starting values for MCMC. Here we focused on the implementation of quantile binary regression and negative binomial regression, but any similar latent variable approach can be incorporated just as easily. A known downside of these approaches, beyond the fact that some carry a large computational cost, is that in certain situations (such as when binary data is heavily imbalanced) there can be severe autocorrelation in the MCMC posterior samples due to the close relationship between the parameters and the latent variables, and may be outperformed by a Metropolis-Hastings approach (Johndrow et al., 2018). Zens et al. (2023) proposed using parameter expansion (Liu and Wu, 1999) to improve the efficiency of fitting a logistic regression model via Polya-Gamma latent variables (Polson et al., 2013). Duan et al. (2018) suggest improvements to the efficiency by scaling the conditional posterior variance; these methods and others can be incorporated to the DLM framework used here if desired.

Beyond the concerns around how the model is fit, we must also consider the model itself and its validity in capturing lag-response dynamics. In this manuscript we focused purely on b-splines to model the lag-response. These are extremely easy to fit as they are simply linear predictors like any other; a similar (though overly-parameterised approach) would be to include the raw lags as predictors. However the disadvantage of these approaches are the potentially irreconcilable interpretations of the fitted model; using linear predictors to model the lag-response, it is possible that a fitted model may say that a treatment is both beneficial *and* detrimental, depending on how far back in time the subject was exposed to it. While there may be some situations where this is a reasonable outcome, we cannot imagine a scenario where that would be true for the effect of air quality exposure to human health, a topic where these models are commonly applied. Functional constraints on the lag response such as distributed lag functions often encountered in MIDAS model literature, can rectify this. Even a simple two parameter model, such as (4) can be enough to model the delayed nature of accumulating lag-response, *and* enforce mono-directional lag effects. The drawback is that they are more difficult to fit, as the full-conditional distribution of the parameters are sampling-intractable. Also, since the DLF parameters are linked to each variable and disappear from the model when the associated predictors are removed, they need to be given special consideration during variable inclusion update proposals, i.e. the ‘birth’ and ‘death’ process (Green, 1995; Green and Hastie, 2009).

All relevant code for this manuscript can be found in the following link: [https:](https://)

[//github.com/DanDempsey/Latent-Variable-DLM-Project/tree/main/Code](https://github.com/DanDempsey/Latent-Variable-DLM-Project/tree/main/Code).

Acknowledgements

Daniel Dempsey's work was funded by an Irish Research Council Enterprise Partnership Scheme Award EPSPG/2017/304. Jason Wyse's work was partially supported through a Science Foundation Ireland Frontiers for the Future Award 21/FFP-P/10123 and the European Union's Horizon 2020 research and innovation programme under the Marie Skłodowska-Curie grant agreement No. 813545.

References

Albert, J. H. and Chib, S. (1993). Bayesian Analysis of Binary and Polychotomous Response Data. *Journal of the American Statistical Association*, 88(422):669–679.

Almon, S. (1965). The distributed lag between capital appropriations and expenditures. *Econometrica: Journal of the Econometric Society*, pages 178–196.

Antonelli, J., Wilson, A., and Coull, B. (2021). Multiple exposure distributed lag models with variable selection.

Benoit, D. F. and den Poel, D. V. (2017). bayesQR: A Bayesian Approach to Quantile Regression. *Journal of Statistical Software*, 76(1):1–32.

Benoit, D. F. and Van den Poel, D. (2012). Binary quantile regression: a bayesian approach based on the asymmetric laplace distribution. *Journal of Applied Econometrics*, 27(7):1174–1188.

Buckingham-Jeffery, E., Morbey, R., House, T., Elliot, A. J., Harcourt, S., and Smith, G. E. (2017). Correcting for day of the week and public holiday effects: improving a national daily syndromic surveillance service for detecting public health threats. *BMC Public Health*, 17(1):1–9.

Carvalho, C. M., Polson, N. G., and Scott, J. G. (2010). The horseshoe estimator for sparse signals. *Biometrika*, 97(2):465–480.

Chen, D., Courtney, R., and Schmitz, A. (1972). A polynomial lag formulation of milk production response. *American Journal of Agricultural Economics*, 54(1):77–83.

Chipman, H. A., George, E. I., and McCulloch, R. E. (2010). BART: Bayesian additive regression trees. *The Annals of Applied Statistics*, 4(1):266 – 298.

Clements, M. P. and Galvão, A. B. (2008). Macroeconomic forecasting with mixed-frequency data. *Journal of Business & Economic Statistics*, 26(4):546–554.

Czado, C. and Santner, T. J. (1992). The effect of link misspecification on binary regression inference. *Journal of statistical planning and inference*, 33(2):213–231.

D’Angelo, L. and Canale, A. (2022). Efficient posterior sampling for bayesian poisson regression. *arXiv preprint arXiv:2109.09520*.

Dhrymes, P. J. (1981). *Distributed lags; problems of estimation and formulation*, volume 2. Holden-Day.

Duan, L. L., Johndrow, J. E., and Dunson, D. B. (2018). Scaling up data augmentation mcmc via calibration. *The Journal of Machine Learning Research*, 19(1):2575–2608.

Frühwirth-Schnatter, S. and Frühwirth, R. (2010). Data augmentation and mcmc for binary and multinomial logit models. *Statistical modelling and regression structures: Festschrift in honour of Ludwig Fahrmeir*, pages 111–132.

Gasparrini, A. (2011). Distributed lag linear and non-linear models in R: the package dlnm. *Journal of Statistical Software*, 43(8):1–20.

Ghysels, E., Kvedaras, V., and Zemlys, V. (2016). Mixed Frequency Data Sampling Regression Models: The R Package midasr. *Journal of Statistical Software*, 72(1):1–35.

Ghysels, E., Santa-Clara, P., and Valkanov, R. (2004). The midas touch: Mixed data sampling regression models. *UCLA: Finance*.

Green, P. and Hastie, D. (2009). Reversible jump MCMC. *Genetics*, 155.

Green, P. J. (1995). Reversible Jump Markov Chain Monte Carlo Computation and Bayesian Model Determination. *Biometrika*, 82(4):711–732.

Hannan, E. J. (1965). The estimation of relationships involving distributed lags. *Econometrica: Journal of the Econometric Society*, pages 206–224.

Hastie, T. and Tibshirani, R. (1987). Generalized additive models: some applications. *Journal of the American Statistical Association*, 82(398):371–386.

Holmes, C. C. and Held, L. (2006). Bayesian auxiliary variable models for binary and multinomial regression. *Bayesian Analysis*, 1(1):145–168.

Johndrow, J. E., Smith, A., Pillai, N., and Dunson, D. B. (2018). Mcmc for imbalanced categorical data. *Journal of the American Statistical Association*.

Jorgensen, B. (2012). *Statistical properties of the generalized inverse Gaussian distribution*, volume 9. Springer Science & Business Media.

Kozumi, H. and Kobayashi, G. (2011). Gibbs sampling methods for Bayesian quantile regression. *Journal of Statistical Computation and Simulation*, 81(11):1565–1578.

Li, X., Yu, H., Xie, Y., and Li, J. (2021). Attention-based novel neural network for mixed frequency data. *CAAI Transactions on Intelligence Technology*, 6(3):301–311.

Liu, J. S. and Wu, Y. N. (1999). Parameter expansion for data augmentation. *Journal of the American Statistical Association*, 94(448):1264–1274.

Meier, L., Van De Geer, S., and Bühlmann, P. (2008). The group lasso for logistic regression. *Journal of the Royal Statistical Society: Series B (Statistical Methodology)*, 70(1):53–71.

Mitchell, T. J. and Beauchamp, J. J. (1988). Bayesian variable selection in linear regression. *Journal of the american statistical association*, 83(404):1023–1032.

Mogliani, M. and Simoni, A. (2020). Bayesian MIDAS Penalized Regressions: Estimation, Selection, and Prediction. *arXiv:1903.08025 [econ]*.

Mork, D., Kioumourtzoglou, M.-A., Weisskopf, M., Coull, B. A., and Wilson, A. (2021). Heterogeneous distributed lag models to estimate personalized effects of maternal exposures to air pollution. *arXiv preprint arXiv:2109.13763*.

Piironen, J. and Vehtari, A. (2017). Sparsity information and regularization in the horseshoe and other shrinkage priors. *Electronic Journal of Statistics*, 11(2):5018 – 5051.

Pillow, J. and Scott, J. (2012). Fully bayesian inference for neural models with negative-binomial spiking. *Advances in neural information processing systems*, 25.

Polson, N. G., Scott, J. G., and Windle, J. (2013). Bayesian Inference for Logistic Models Using Pólya-Gamma Latent Variables. *Journal of the American Statistical Association*, 108(504):1339–1349.

Schwartz, J. (2000). The Distributed Lag between Air Pollution and Daily Deaths. *Epidemiology*, 11(3):320–326.

Sims, C. A. (1971). Discrete approximations to continuous time distributed lags in econometrics. *Econometrica: Journal of the Econometric Society*, pages 545–563.

van Buuren, S. and Groothuis-Oudshoorn, K. (2011). mice: Multivariate imputation by chained equations in r. *Journal of Statistical Software*, 45(3):1–67.

Warren, J. L., Luben, T. J., and Chang, H. H. (2020). A spatially varying distributed lag model with application to an air pollution and term low birth weight study. *Journal of the Royal Statistical Society. Series C, Applied statistics*, 69(3):681.

Wilson, A., Chiu, Y.-H. M., Hsu, H.-H. L., Wright, R. O., Wright, R. J., and Coull, B. A. (2017). Bayesian distributed lag interaction models to identify perinatal windows of vulnerability in children’s health. *Biostatistics*, 18(3):537–552.

Xu, Q., Zhuo, X., Jiang, C., and Liu, Y. (2019). An artificial neural network for mixed frequency data. *Expert Systems with Applications*, 118:127–139.

Xu, X. and Ghosh, M. (2015). Bayesian variable selection and estimation for group lasso. *Bayesian Analysis*, 10(4):909–936.

Yu, K. and Zhang, J. (2005). A Three-Parameter Asymmetric Laplace Distribution and Its Extension. *Communications in Statistics - Theory and Methods*, 34(9-10):1867–1879.

Zanobetti, A., Schwartz, J., Samoli, E., Gryparis, A., Touloumi, G., Atkinson, R., Le Tertre, A., Bobros, J., Celko, M., Goren, A., et al. (2002). The temporal pattern of mortality responses to air pollution: a multicity assessment of mortality displacement. *Epidemiology*, pages 87–93.

Zens, G., Frühwirth-Schnatter, S., and Wagner, H. (2023). Ultimate p\’olya gamma samplers—efficient mcmc for possibly imbalanced binary and categorical data. *arXiv preprint arXiv:2011.06898*.

Zhou, M., Li, L., Dunson, D., and Carin, L. (2012). Lognormal and gamma mixed negative binomial regression. In *Proceedings of the... International Conference on Machine Learning. International Conference on Machine Learning*, volume 2012, page 1343. NIH Public Access.

Bayesian Generalized Distributed Lag Regression with Variable Selection: Supplemental Material

Daniel Dempsey and Jason Wyse

Negative Binomial Simulation Results

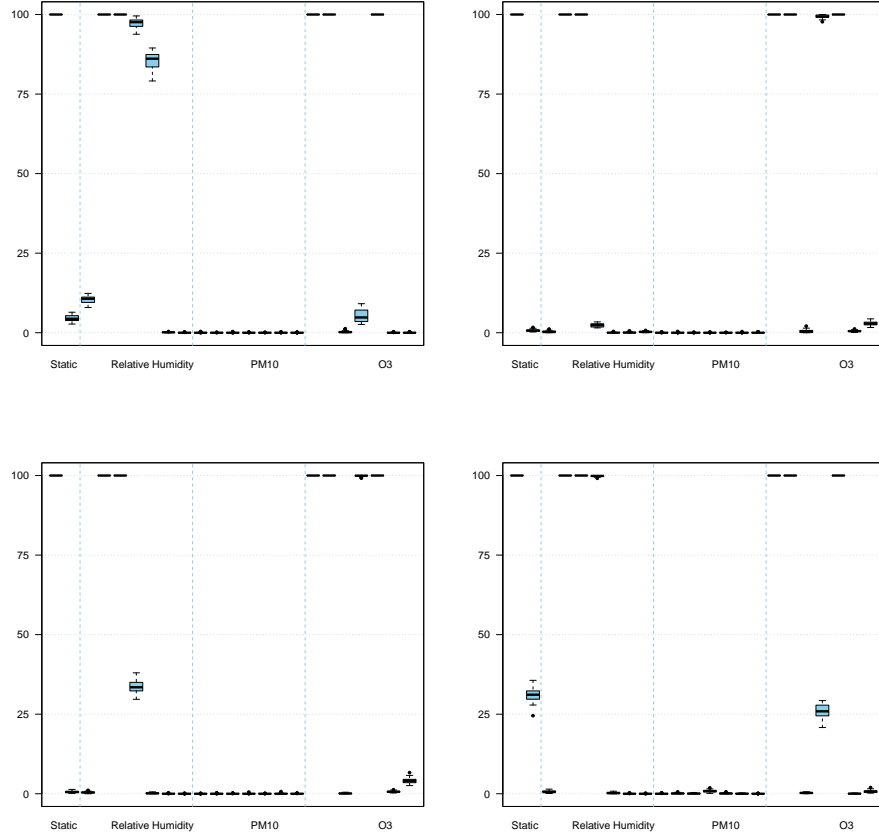


Figure 1: Covariate inclusion parameters for large simulations.

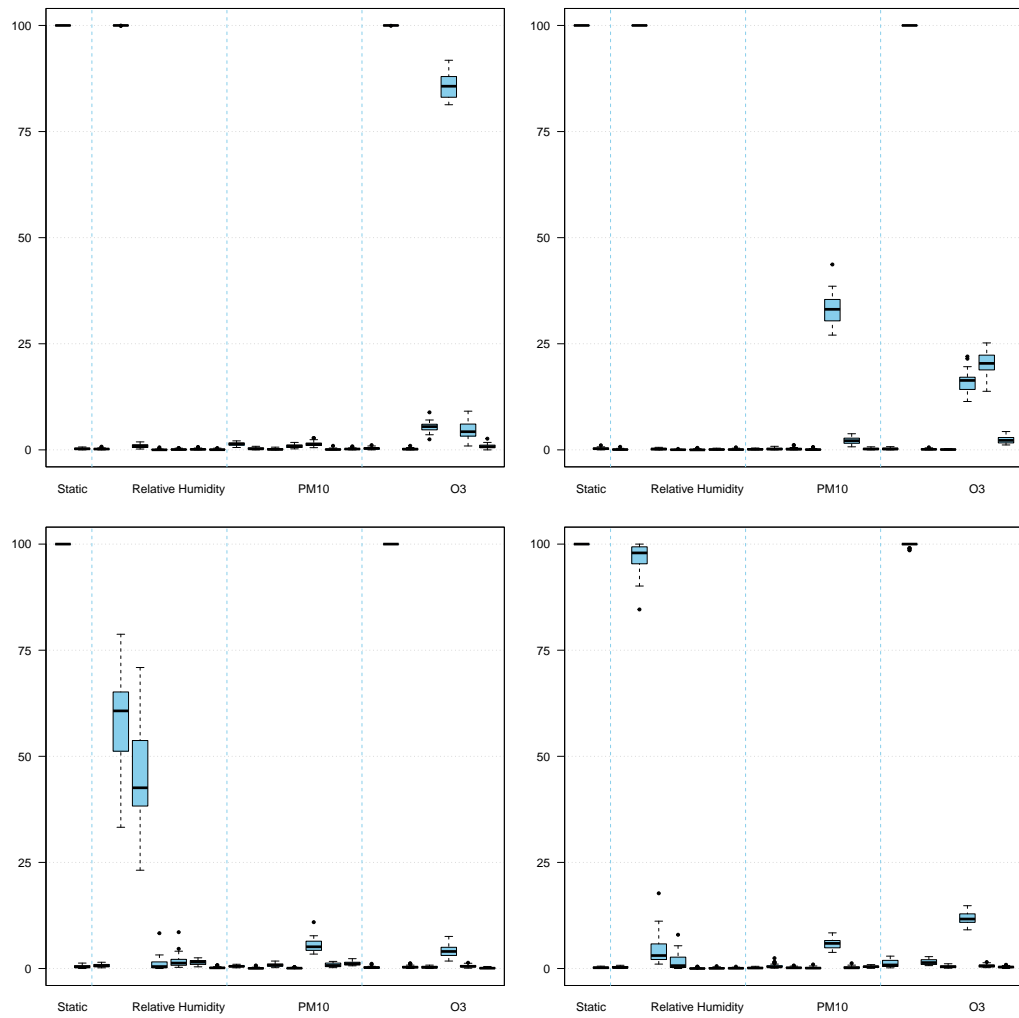


Figure 2: Covariate inclusion parameters for small simulations.

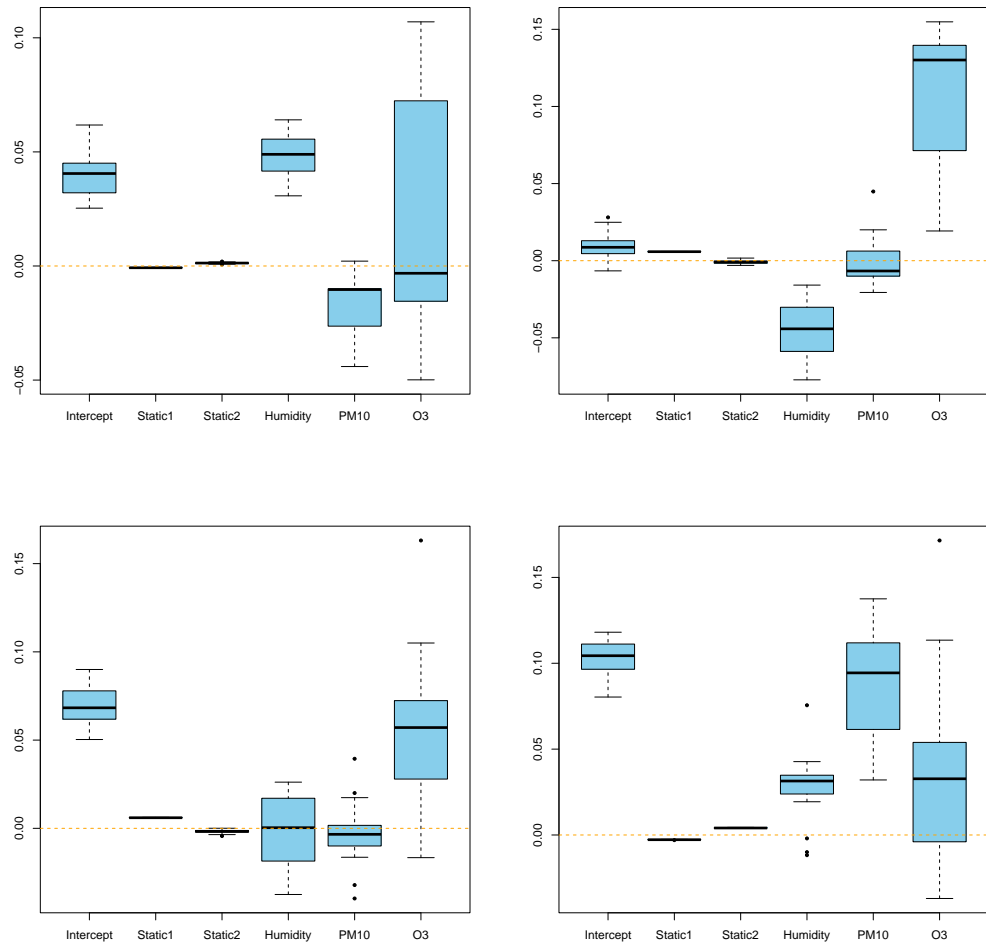


Figure 3: Slope parameters for large simulations.

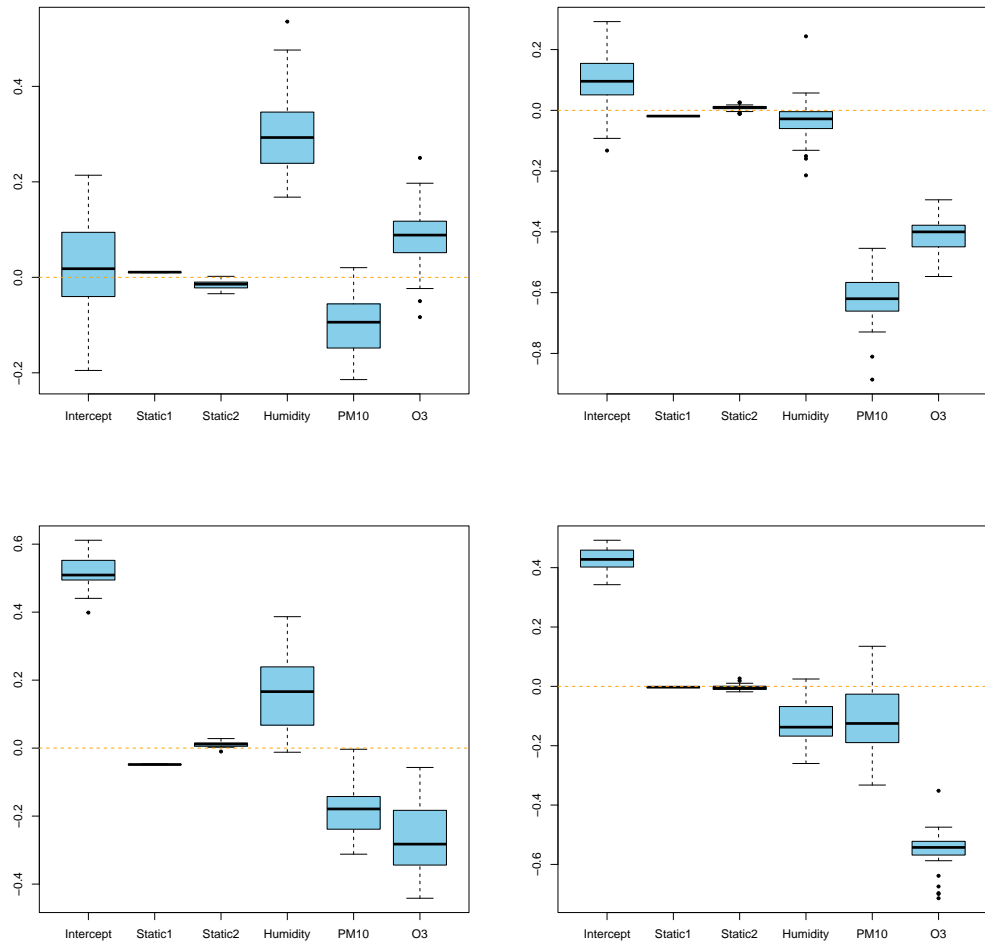


Figure 4: Slope parameters for small simulations.

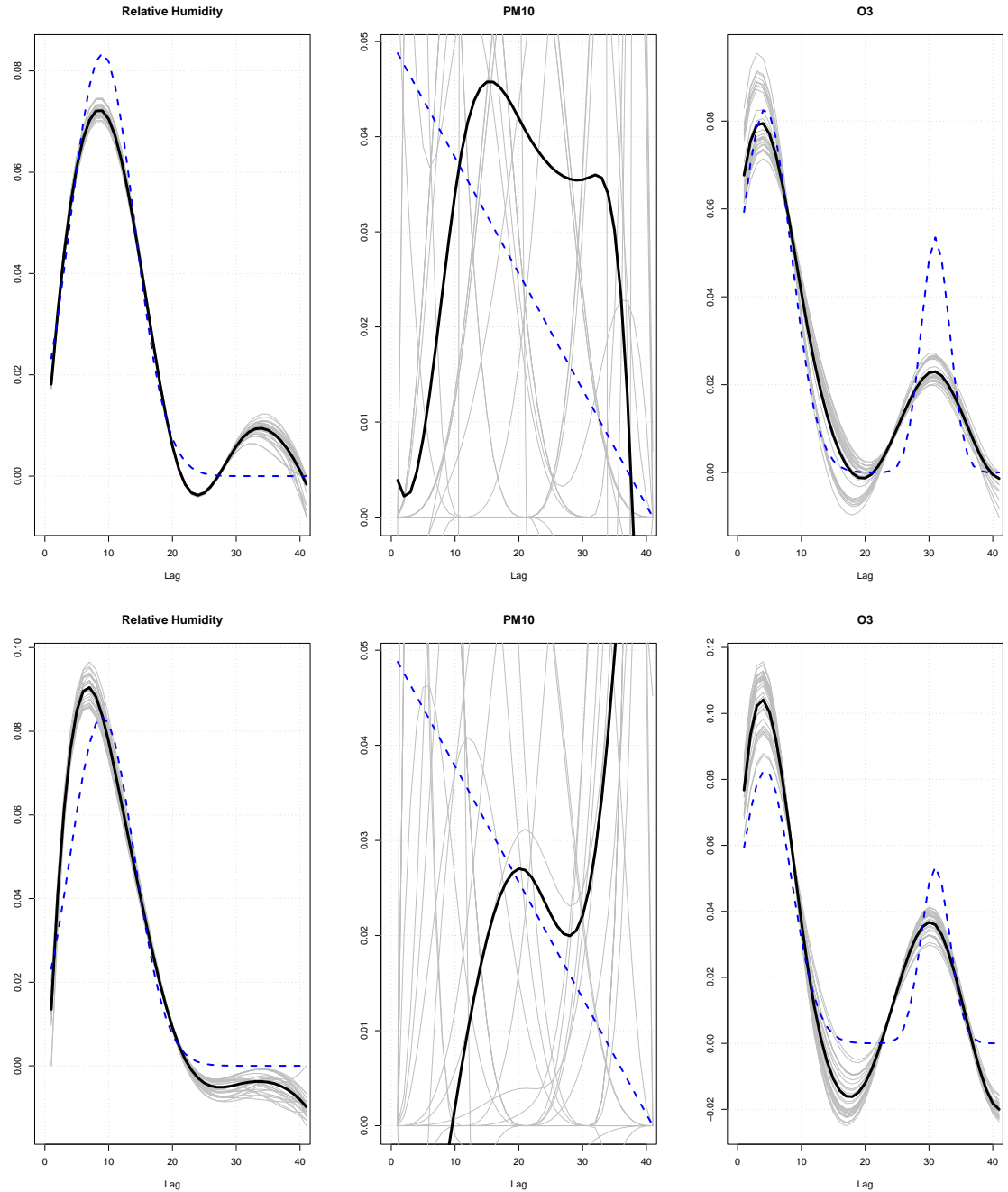


Figure 6: Estimated lag-response for the first and second large simulations.

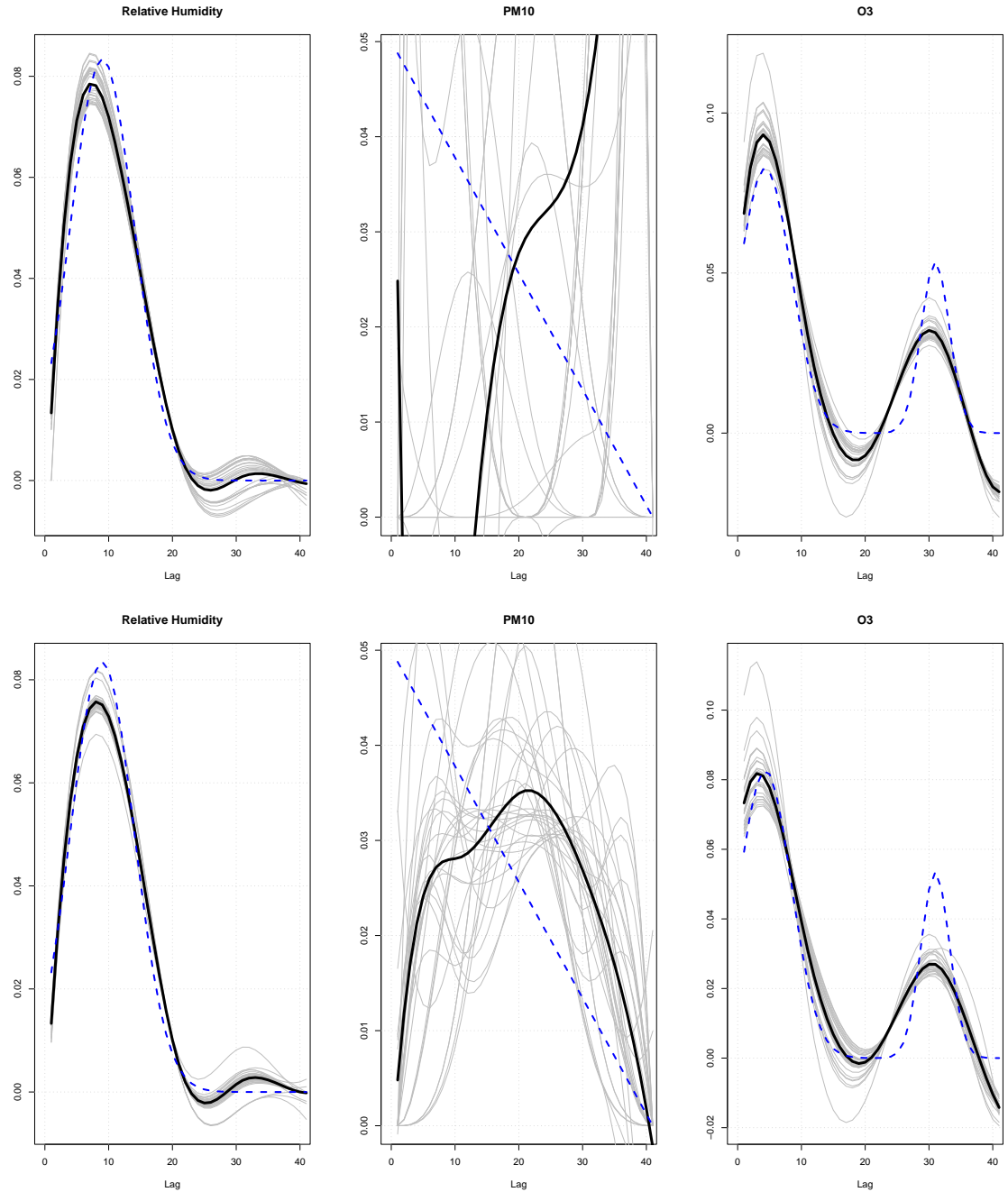


Figure 8: Estimated lag-response for the third and fourth large simulations.

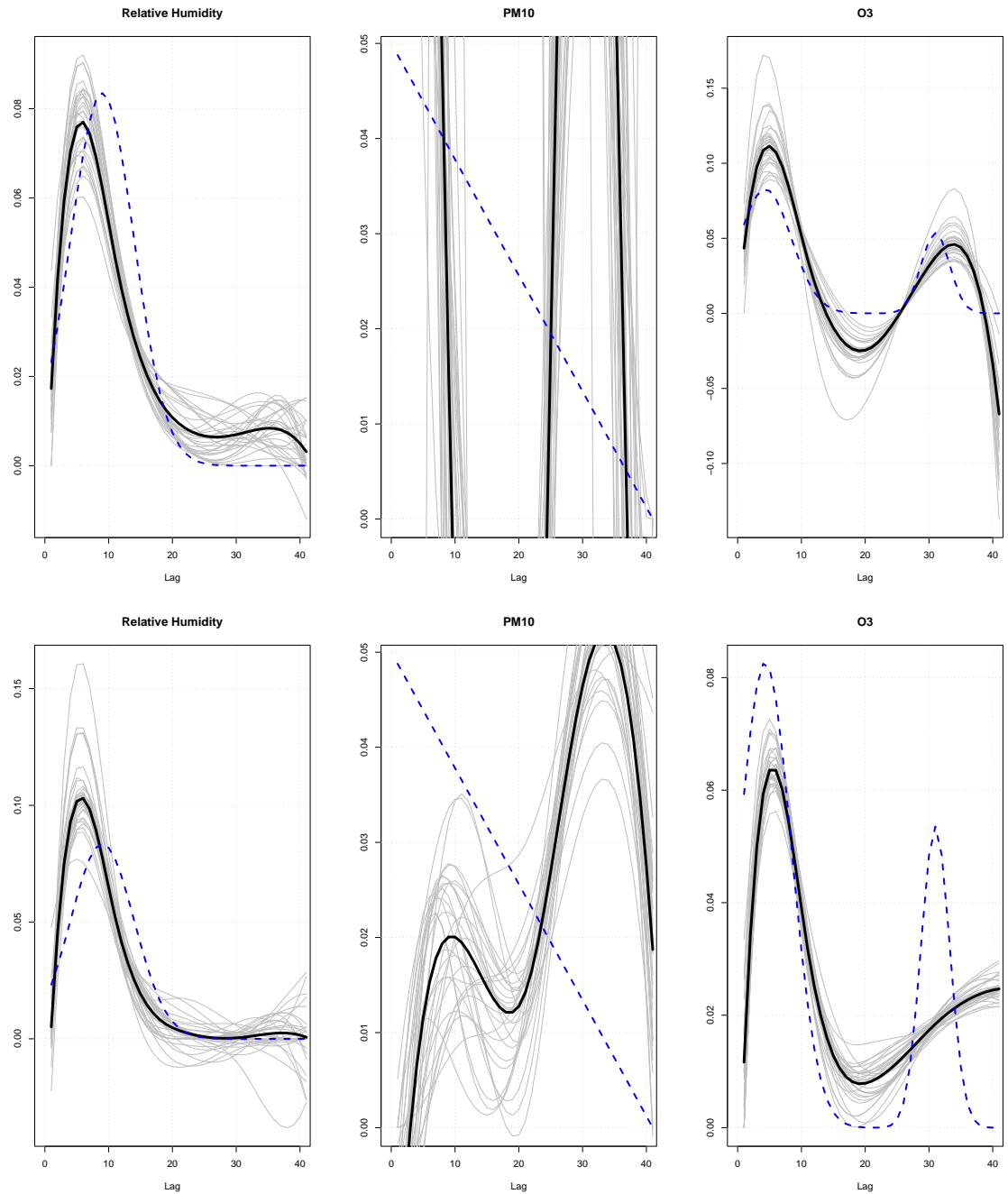


Figure 10: Estimated lag-response for the first and second small simulations.

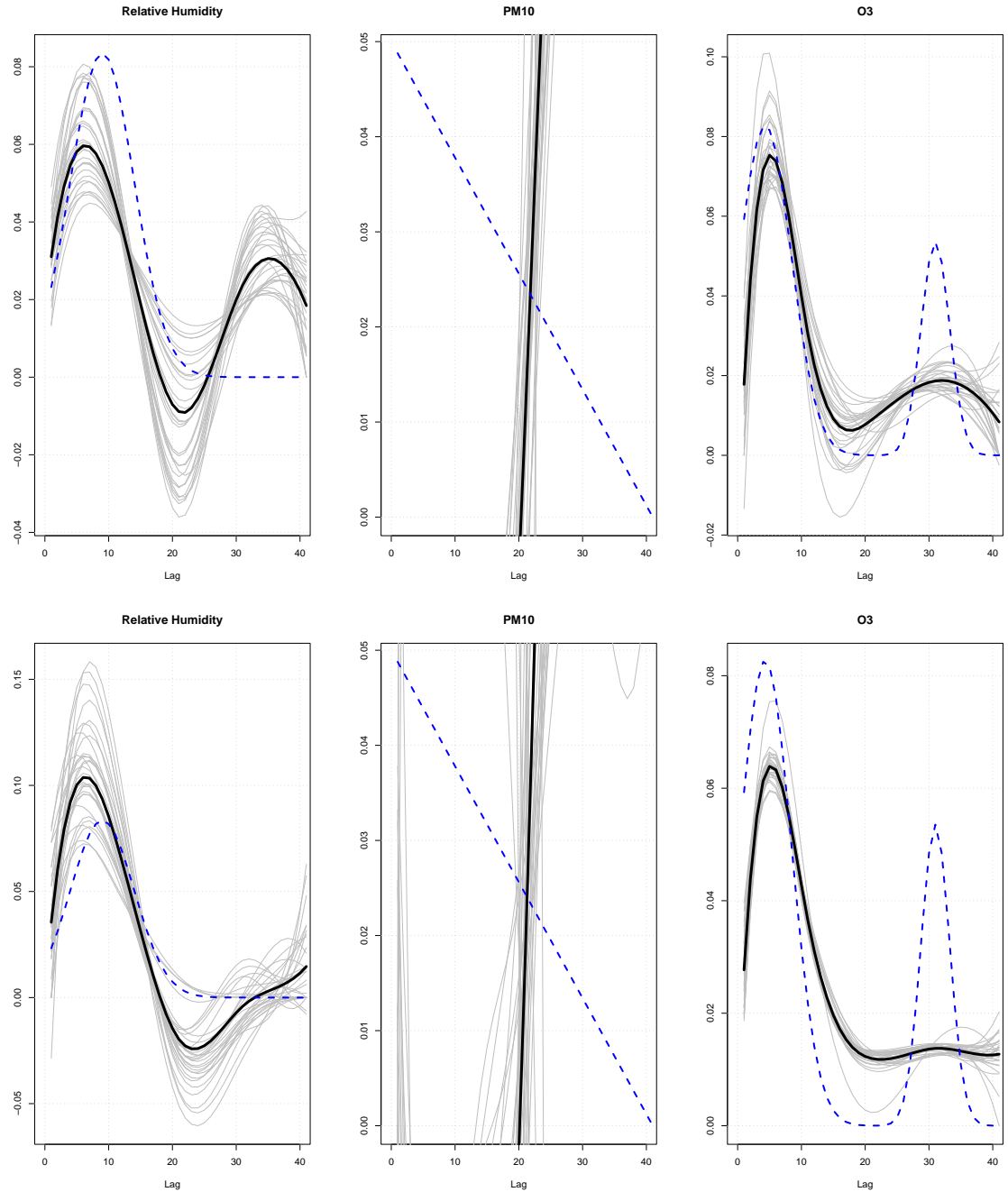


Figure 12: Estimated lag-response for the third and fourth small simulations.

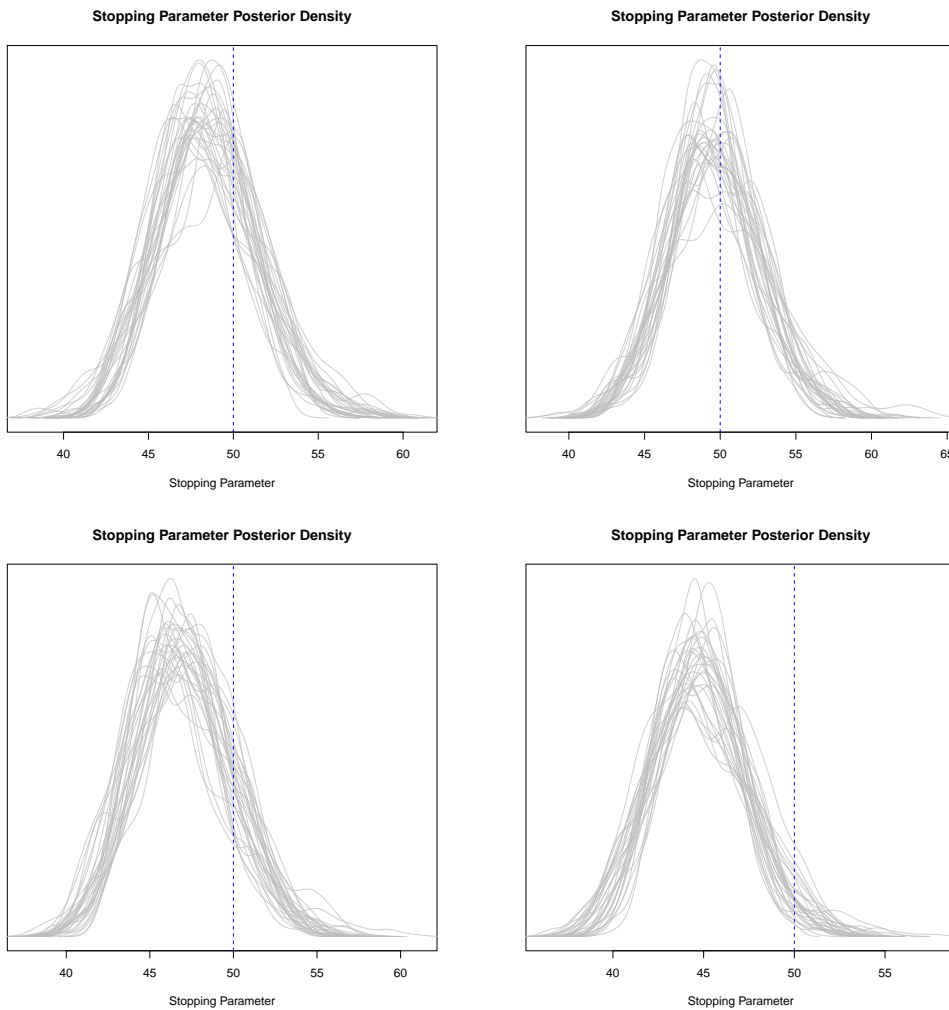


Figure 13: Stopping parameter posteriors for large simulations.

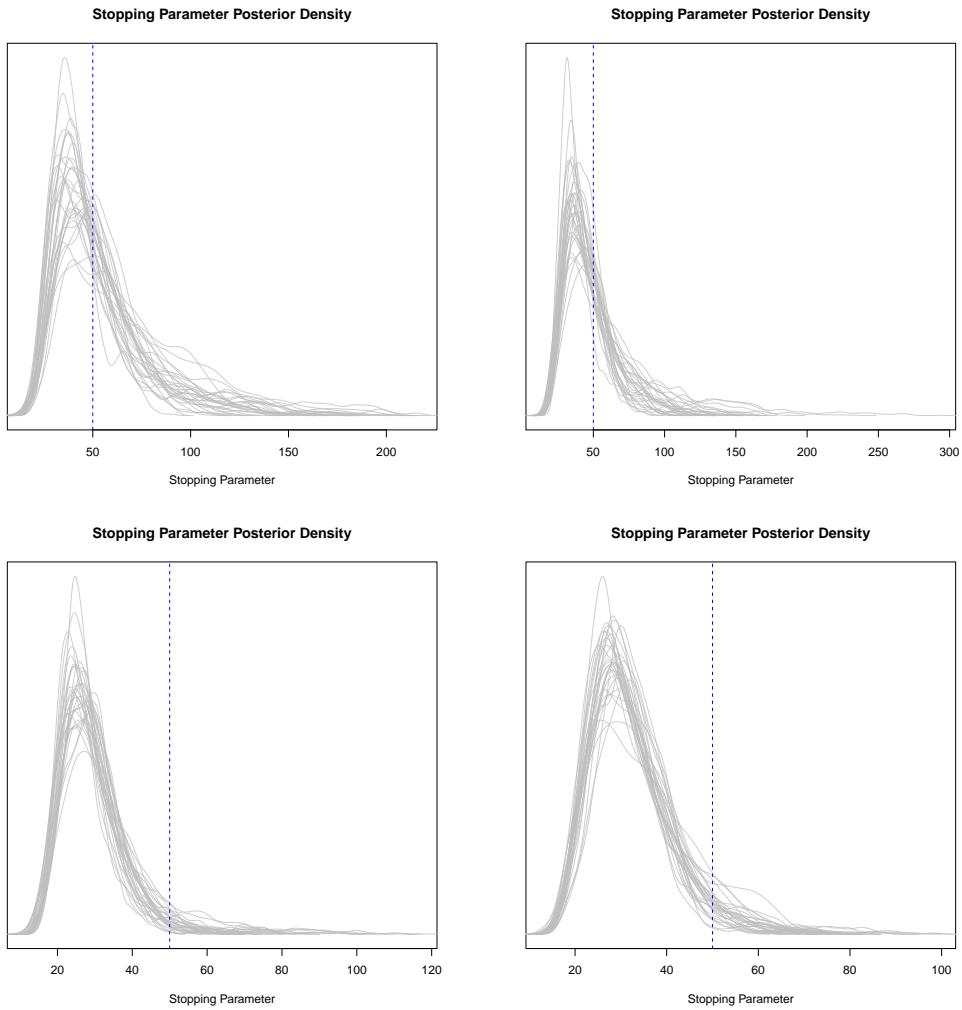


Figure 14: Stopping parameter posteriors for small simulations.

Quantile Binary Simulation Results

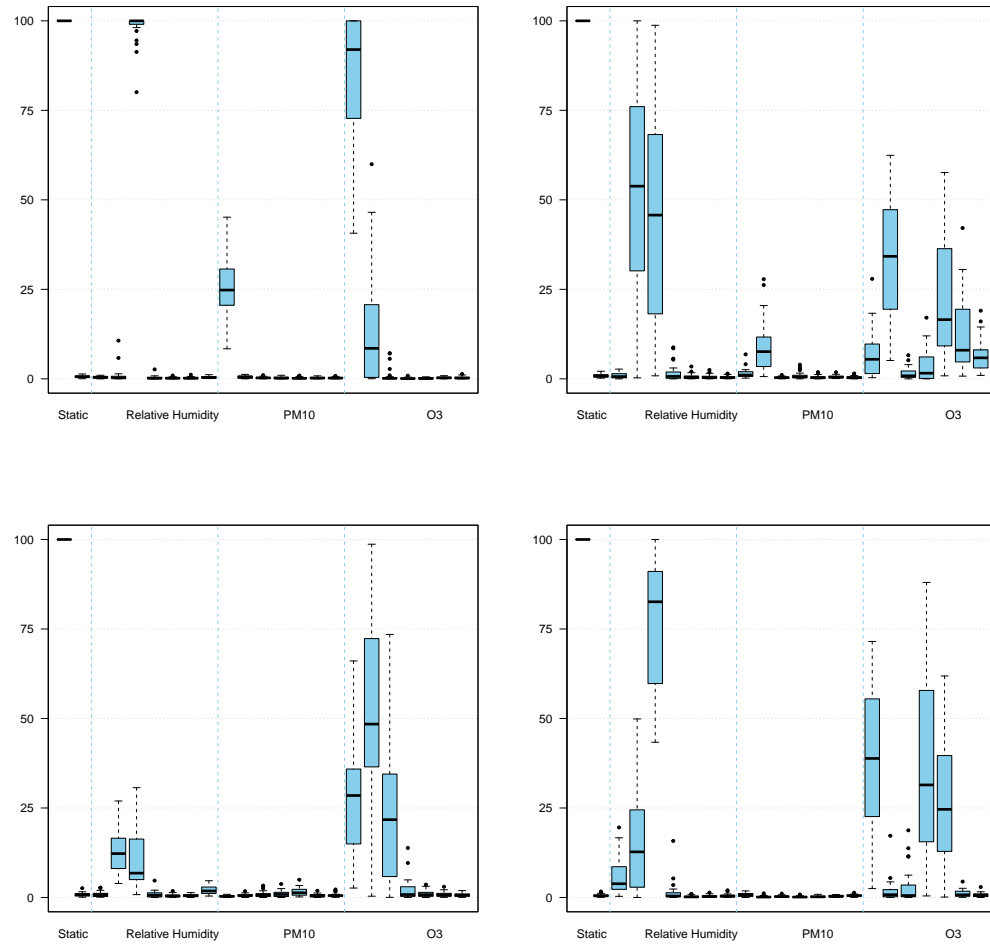


Figure 15: Covariate inclusion parameters for large simulations.

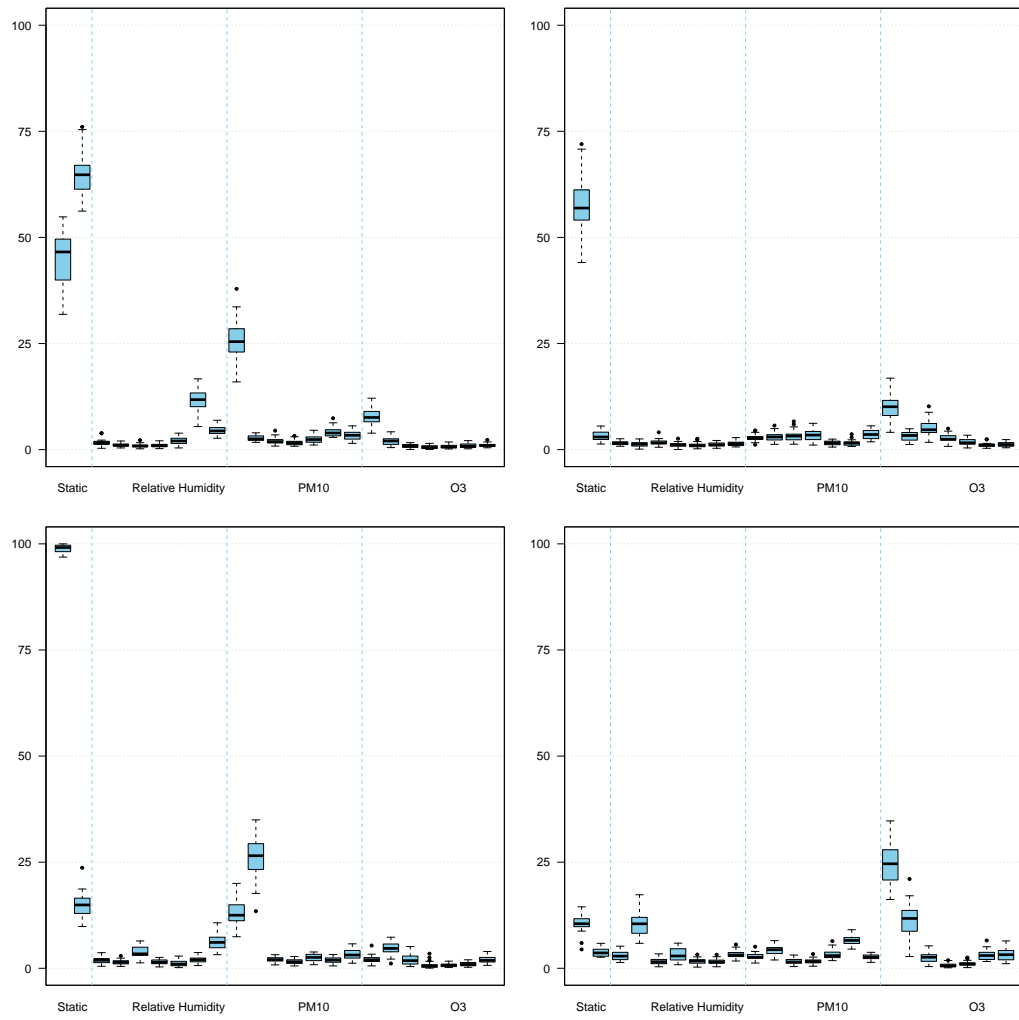


Figure 16: Covariate inclusion parameters for small simulations.

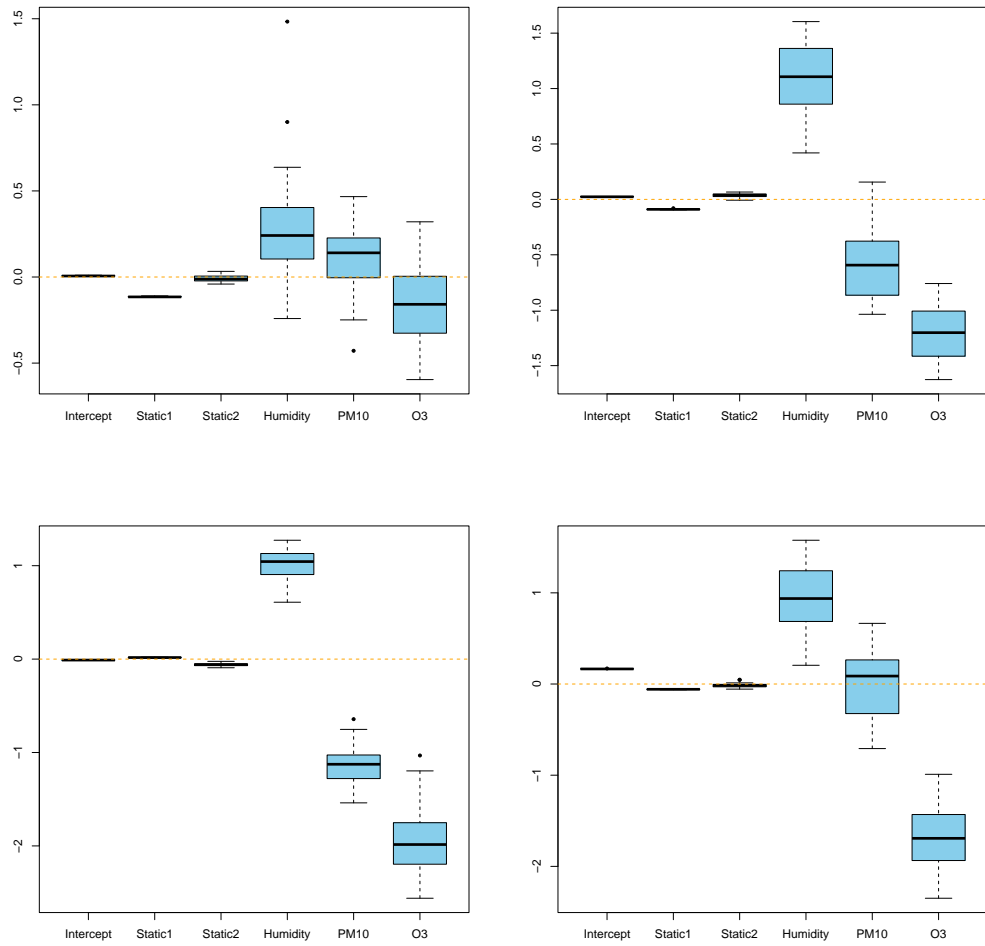


Figure 17: Slope parameters for large simulations.

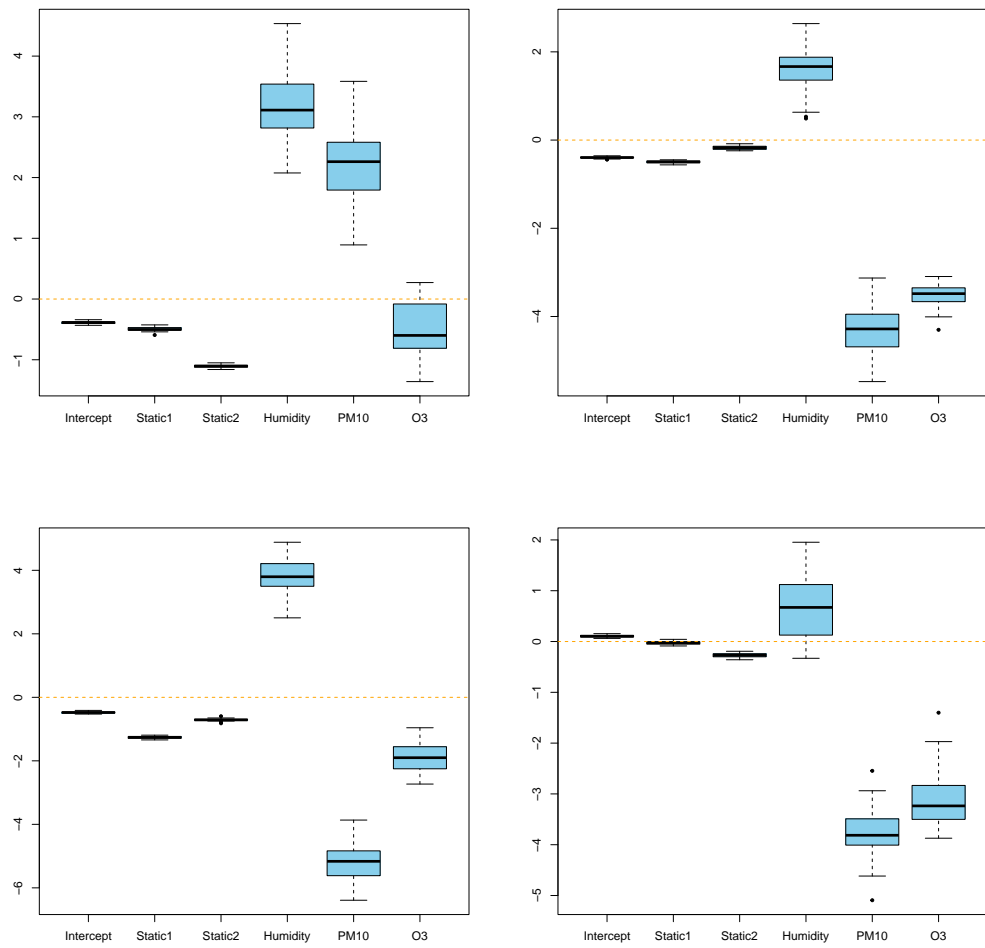


Figure 18: Slope parameters for small simulations.

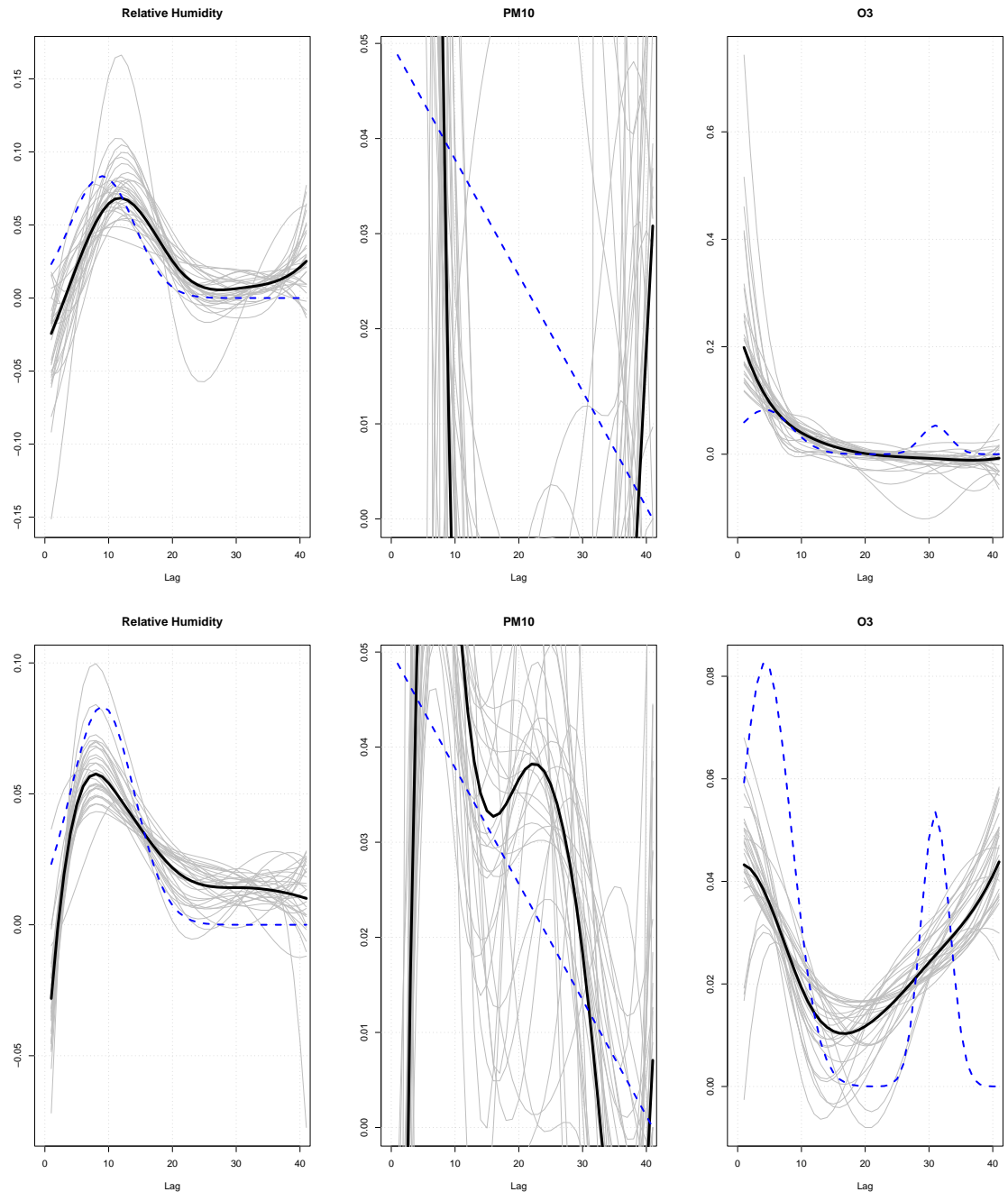


Figure 20: Estimated lag-response for the first and second large simulations.

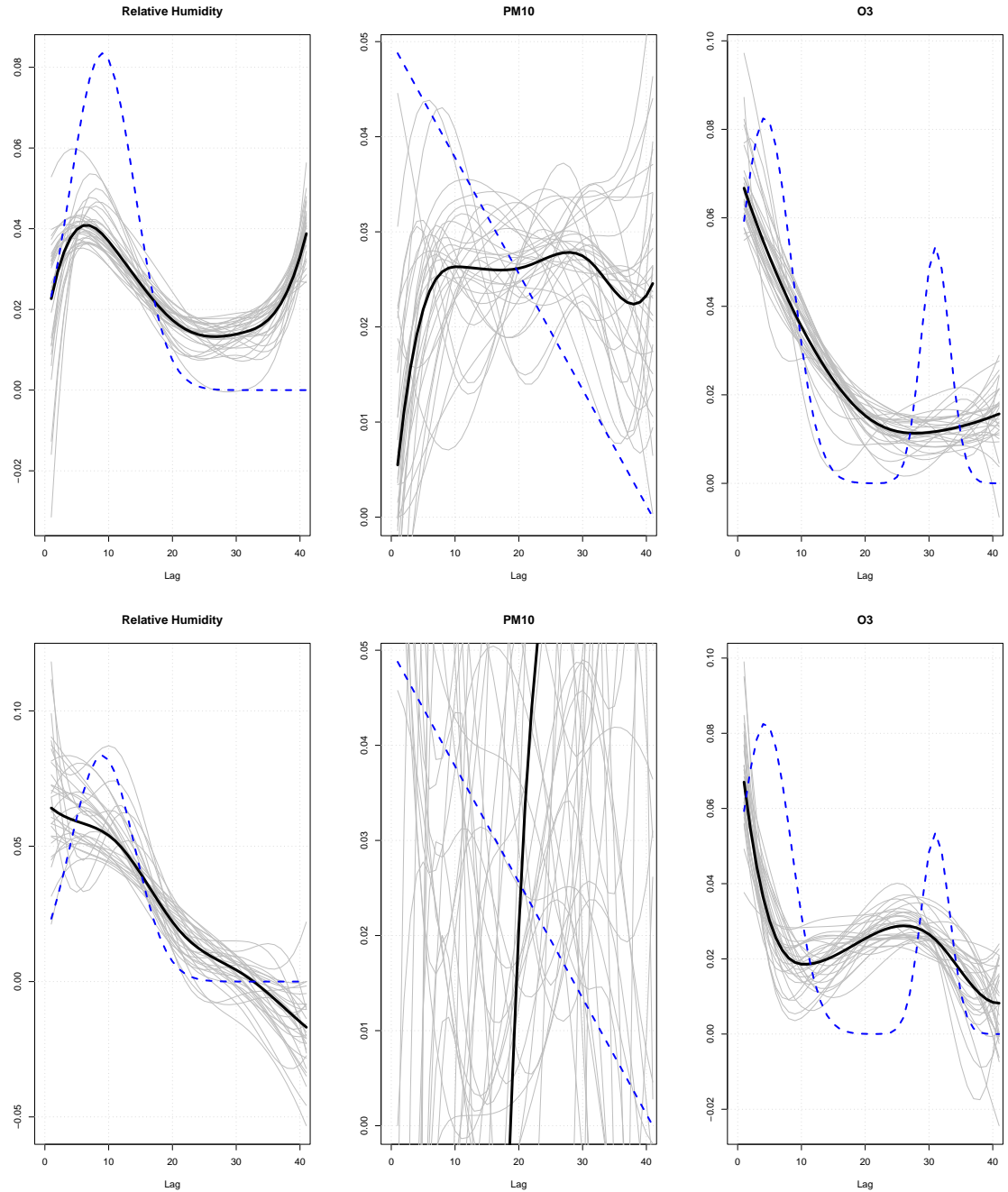


Figure 22: Estimated lag-response for the third and fourth large simulations.

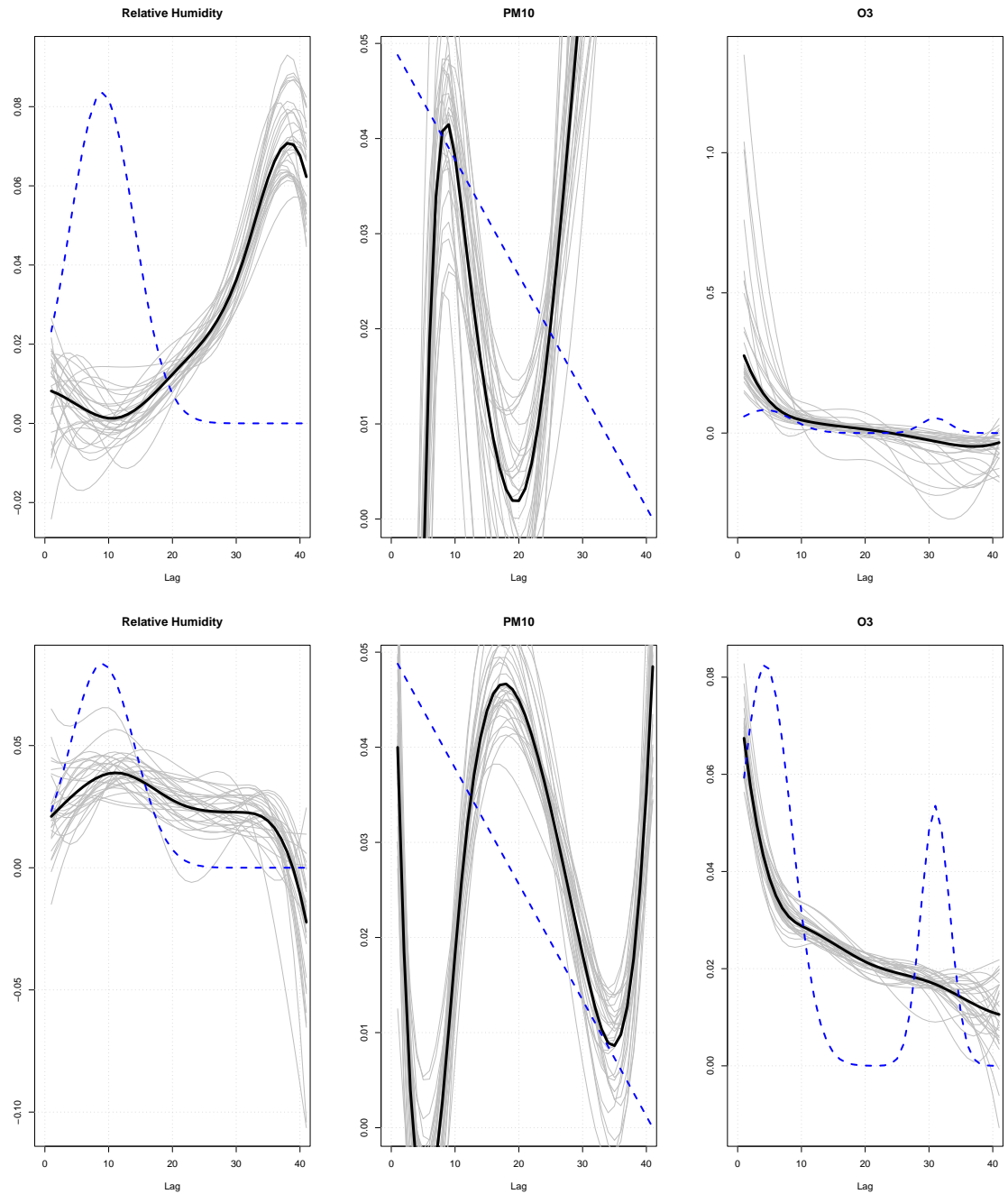


Figure 24: Estimated lag-response for the first and second small simulations.

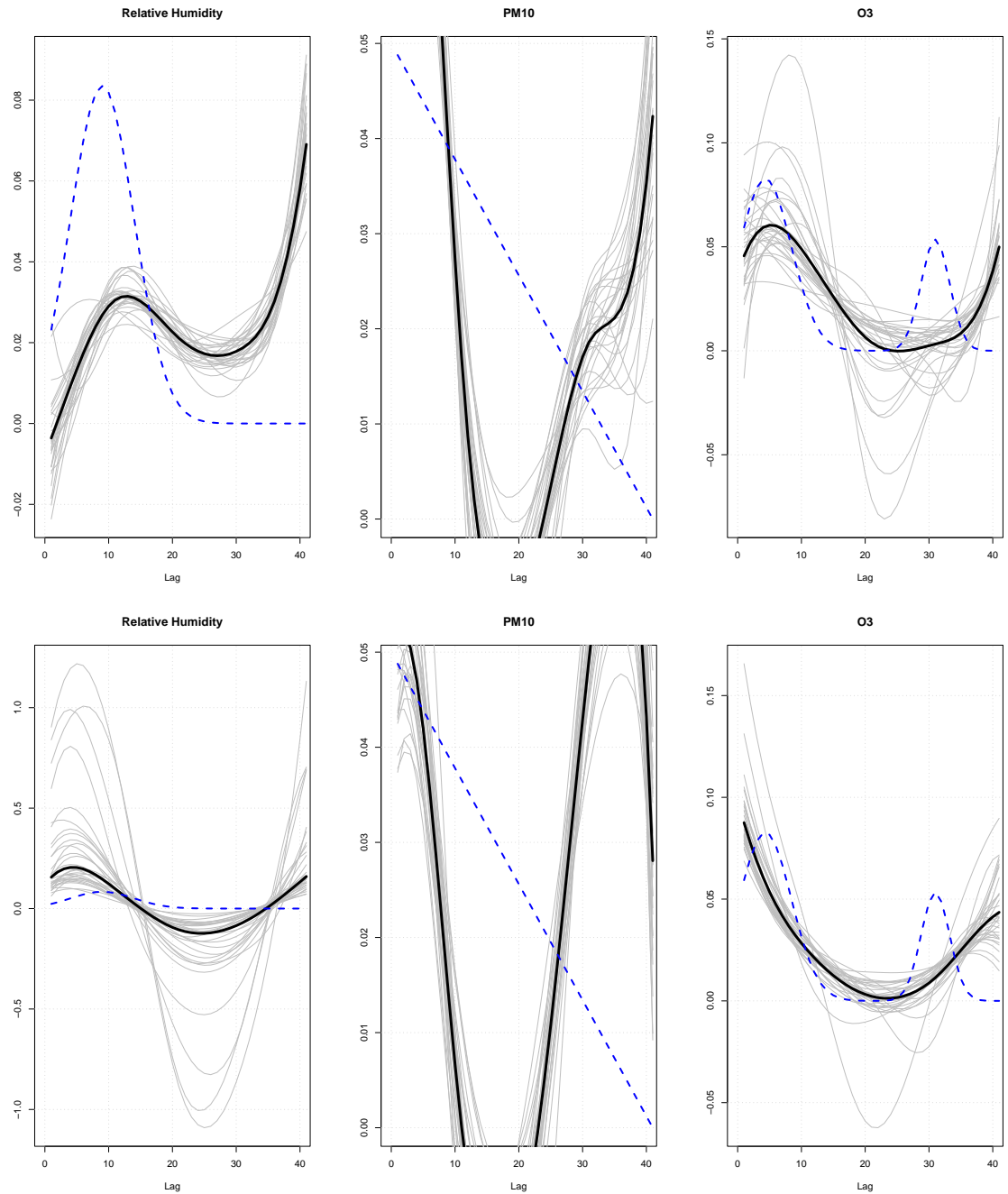


Figure 26: Estimated lag-response for the third and fourth small simulations.